Microb Ecol (2011) 62:655–668
DOI 10.1007/s00248-011-9855-2

MICROBIOLOGY OF AQUATIC SYSTEMS

Diversity and Spatial Distribution of Prokaryotic Communities Along A Sediment Vertical Profile of A Deep-Sea Mud Volcano

Maria G. Pachiadaki · Argyri Kallionaki · Anke Dählmann · Gert J. De Lange · Konstantinos Ar. Kormas

Received: 7 December 2010 / Accepted: 6 April 2011 / Published online: 3 May 2011

Abstract We investigated the top 30-cm sediment prokaryotic community structure in 5-cm spatial resolution, at an active site of the Amsterdam mud volcano, East Mediterranean Sea, based on the 16S rRNA gene diversity. A total of 339 and 526 sequences were retrieved, corresponding to 25 and 213 unique (≥98% similarity) phylotypes of Archaea and Bacteria, respectively, in all depths. The Shannon–Wiener diversity index H was higher for Bacteria (1.92–4.03) than for Archaea (0.99–1.91) and varied differently between the two groups. Archaea were dominated by anaerobic methanotrophs ANME-1, -2 and -3 groups and were related to phylotypes involved in anaerobic oxidation of methane from similar habitats. The much more complex Bacteria community consisted of 20 phylogenetic groups at the phylum/candidate division level. *Proteobacteria*, in particular *δ-Proteobacteria*, was the dominant group. In most sediment layers, the dominant phylotypes of both the Archaea and Bacteria communities were found in neighbouring layers, suggesting some overlap in species richness. The similarity of certain prokaryotic communities was also depicted by using four different similarity indices. The direct comparison of the retrieved phylotypes with those from the Kazan mud volcano of the same field revealed that 40.0% of the Archaea and 16.9% of the Bacteria phylotypes are common between the two systems. The majority of these phylotypes are closely related to phylotypes originating from other mud volcanoes, implying a degree of endemicity in these systems.

Electronic supplementary material The online version of this article (doi:10.1007/s00248-011-9855-2) contains supplementary material, which is available to authorized users.

M. G. Pachiadaki · K. A. Kormas (✉)
Department of Ichthyology and Aquatic Environment,
School of Agricultural Sciences, University of Thessaly,
384 46 Volos, Magnesia, Greece
e-mail: kkormas@uth.gr

A. Kallionaki
Environmental Engineering Department,
Technical University of Crete,
73 100 Chania, Crete, Greece

A. Dählmann · G. J. De Lange
Department of Earth Sciences, Utrecht University,
PO Box 80021 3508 TA, Utrecht, The Netherlands

Introduction

Mud volcanoes (MV) are areas of active fluid seepage occurring both on land and at the seafloor [50]. Submarine MV are often associated with the presence of gas hydrates. During the past years, many studies have attempted to address the fate of methane originating from submarine MV, its impact on the global carbon cycle and the role of the in situ microbial communities on the production and the consumption of this potent greenhouse gas [7, 31, 38 and references therein, 55]. Active marine MV could be considered as analogue habitats of fluidized or mobile muds (sensu Aller et al. [1]) since they consist of a mixture of fine-grained, creamy-textured sediment and fluids, expanding down to 1 m or deeper, although these sediments can be remobilized due to irregular and unpredictable eruptions. Such habitats serve as efficient methane and sulfur reactors, hosting characteristically high bacterial and low archaeal diversity. It is expected that MV undergo temporal and spatial changes due to changes in gas/fluid fluxes, eruptions and gas hydrate association–dissociation, probably ensuing successive stages in microbial community structure and functioning.

In the eastern Mediterranean Sea, MV and cold-seep areas were discovered during the late 1970s [13] whilst ongoing research has revealed several such formations on the accretionary prism of the Hellenic Arc (Mediterranean Ridge) and within the Anaximander Mountains [47, 85]. Amsterdam MV (AMSMV) has 'mud pie-like' topography and appears as a circular structure with a flat-topped mound at a water depth on its summit of 2,025 m [46, 87]. Detailed morphological analysis of the AMSMV indicated that there are two discrete craters the 'external' and the 'internal' that merge to the southeast. Both are ellipses with dimensions of 6×5 km and 4×3.3 km, respectively, slightly elongated in an N–S direction. One common morphological characteristic of the craters is that they are both open in the southernmost part and directly connected to the slope with a 400-m wide canyon extending down to a depth of 2,250 m [46].

AMSMV is considered as the largest and most active MV investigated in the Anaximander Mountains field based on the occurring mud breccia. It has been related to moderate to fast ascending fluidized mud and/or a relatively wide conduit [46, 87]. Seismic profiling and side scan sonar surveys across the mud volcanic structure revealed features attributed to recent mud extrusion in the crater and outflow downslope to the south [46, 85, 87]. Support for recent mud volcanic activity is provided from other data as well, such as the rough microtopography, the absence of extended areas with carbonate crusts on the seafloor, the observation of dewatering chimneys and the elevated concentrations of methane in the water column [12, 46, 53, 61, 87]. Active fluid seepage and gas bubble release are common at the summit, particularly in the eastern central part [87].

Considerable near-surface gas hydrate accumulations have been reported for several sites at the AMSMV, particularly close to the MV centre and its eastern sector [46, 61, 87]. High hydrostatic pressure, moderate bottom water temperatures (14.0°C), comparably high water activity and methane oversaturation generally favour gas hydrates to precipitate in shallow deposits of the AMSMV centre [61]. During eruptive phases, however, fluids from below might transport additional heat, leading to increases in temperatures exceeding hydrate dissociation temperatures in deposits covering the investigated depth interval. Compelling evidence support the theory of hydrate destabilisation at shallow sub bottom depths, mainly ^{18}O enrichments of authigenic carbonates [2] and the high methane values in water above the AMSMV [12].

Although AMSMV is the largest MV in the Anaximander field, the microbial communities living in its active sediments have not yet been thoroughly characterised. However, there are a few studies providing evidence for the occurrence of anaerobic oxidation of methane (AOM) in AMSMV, based on the presence of specific lipid biomarkers and carbon isotopic signatures in carbonate crusts [2, 8] and in sediments [59, 60]. Only one study has used the construction of 16S rRNA gene libraries to reveal the inhabitants of AMSMV [29] but the studied sediment was away from the active site of the MV. We aimed at investigating the degree of vertical stratification or overlap between prokaryotic communities occurring in the active site of the AMSMV and how these communities are related to the prevailing geochemistry. To do so, we analysed the communities of Bacteria and Archaea at the top 30-cm sediment of an active site in the AMSMV. Subsamples were taken every 5 cm and features of community structure based on 16S rRNA gene diversity were analysed. Moreover, we investigated possible spatial similarities between similar, but distant to each other, environments, and whether there are common phylotypes which are specific to mud volcanoes habitats.

Materials and Methods

Sampling Site

Box-core AN05BC05 with gas hydrate-containing sediment was collected from the AMSMV (35°20′02″ N, 30°16′18″ E) of the Anaximander Mountains, eastern Mediterranean Sea, with the R/V AEGEO in May 2003. Sediment sampling was conducted as described in [41]. In the current work, the prokaryotic diversity at 0, 5, 10, 15, 20, 25 and 30 cm below sea floor (cm.b.s.f.) was analysed. The detailed description of the geological setting and the geological parameters of the sampled site are reported in [46] whilst the concentrations of methane and sulfate were determined as described in [41]. In brief, samples for porewater extraction of box core sediments were taken immediately upon recovery into Greiner centrifuge tubes and were centrifuged for 20 min at 4,000 rpm. Subsequently, the tightly closed centrifuge tubes were transferred immediately in an oxygen-free glovebox, for filtering (0.2 μm) and subsampling of the porewater samples [for details, see 26]. The subsamples intended for major elements and sulfate analyses were acidified using 25 μl of a 5 M HNO_3 solution per millilitre of porewater.

DNA Extraction, Amplification and Cloning

DNA was extracted from 0.5 to 1 g of sediment from each depth using the UltraClean Soil DNA kit (MoBio Laboratories Inc., USA) following the manufacturer's protocol with minor modifications: bead beating was reduced from 10 to 5 min, and this step was immediately followed by 3 cycles of freeze-and-thaw (−80°C for 3 min and then immediately in 65°C water bath for 5 min) after addition of the inhibitor removal solution. Bacterial 16S rDNA was amplified using the bacterial primers B8f-B1492r [74]. The PCR included an initial denaturation step at 94°C for 1 min

followed by 27 to 31 cycles consisting of denaturation at 94°C for 45 s, annealing at 52.5°C for 45 s, and elongation at 72°C for 2 min; a final 7-min elongation step at 72°C was added. Archaea 16S rDNA was amplified using the primer combination A8f and A1492r [74]. An initial denaturation step at 94°C for 1 min was followed by 25 to 29 cycles consisting of denaturation at 94°C for 45 s, annealing at 52.5°C for 45 s, and elongation at 72°C for 2 min; a final 7-min elongation step at 72°C was added. The number of cycles was determined for each sample after cycle optimisation. PCRs were repeated with different cycle numbers, and the lowest number of cycles that gave a positive signal was then used for cloning and sequencing in order to avoid differential representation of 16S rDNA genes with low and high copy numbers [70]. Eight tubes of PCR products were pooled to reduce the biases of each individual reaction.

Polymerase chain reaction products were visualised on a 1% agarose gel under ultraviolet light, bands were excised, and PCR products were extracted with the Wizard SV Gel and PCR Clean-up kit (Promega Inc., USA) following the manufacturer \primes protocol. The PCR products were cloned using the TOPO TA for sequencing cloning kit (Invitrogen Corporation, USA) using electrocompetent cells according to the manufacturer's specifications. For each sample and each gene, randomly picked clones with inserts of the expected length were analysed. Clones were grown in liquid LB medium with kanamycin and their plasmids were purified using the NucleoSpin Plasmid QuickPure kit (Macherey-Nagel GmbH & Co. KG, Germany) for DNA sequencing. A number of 33–58 and 52–121 of archaeal and bacterial clones (true positives), respectively, were analysed in each sample.

Sequencing and Phylogenetic Analysis

Sequence data were obtained by Macrogen Inc. (South Korea) using capillary electrophoresis and the BigDye Terminator kit (Applied Biosystems Inc., USA) with the primers M13F(−20) and M13R. Every sequence read was approximately 900 bp and for each individual clone, forward and reverse reads were assembled. The sequences were screened for chimaeras by comparing neighbour-joining trees made of the first and second halves of all sequences. The sequences that had different groupings in the first and second halves were then checked using the Pintail programme [4] (http://www.bioinformatics-toolkit.org/Web-Pintail/). Bellerophon software from GreenGenes [17] (http://greengenes.lbl.gov/cgi-bin/nph-bel3_interface.cgi) was also used to detect chimaeric sequences. All putative chimaeras were excluded from further analysis.

For the detection of closest relatives, all sequences were compared with the BLAST function [3] (www.ncbi.nlm.nih.gov/BLAST/). The sequences were automatically aligned against sequences from their closest relatives using SILVA alignment utility [65] (http://www.arb-silva.de/aligner/) and revised by manual removal of ambiguously aligned regions. Phylotypes or operational taxonomic units (OTUs) were defined as sequences showing ≥98% homology to each other.

Phylogenetic trees were constructed by the neighbour-joining method using the Kimura 2-parameter. Bootstrap analyses for 1,000 replicates were performed to assign confidence levels to the tree topology using the MEGA4 software [73]. Sequences of unique phylotypes found in this study have GenBank numbers HQ588634-HQ588688 (Archaea) and HQ588358-HQ588633 (Bacteria).

Clone Library Coverage, Diversity and Similarity Analyses

Clone coverage was calculated using the equation $C=[1-(n_i/N)]\times 100$, where n_i is the number of phylotypes and N is the number of 16S rRNA sequences examined [23, 37]. The Shannon–Wiener index H′ was used as a diversity index and was calculated as follows: $H' = -\sum p_i \cdot \ln p_i$, where the summation is over all phylotypes i, and p_i is the proportion of clones belonging to phylotype i relative to the sum of all clones. The Pielou evenness index J was calculated as $J=H'/\ln S$, where S is the total number of phylotypes [64, 69].

The similarity among the microbial communities in all sediment layers was determined using four different indices of similarity: Morisita-Horn [32], Morisita [52], Jaccard Abundance adjusted and Sorensen Abundance adjusted [11]. Morisita-Horn and Morisita indices were chosen because they are widely applied and unbiased for sample size [84]. The most newly developed indices Jaccard Abundance adjusted and Sorensen Abundance were used as they were proved to be less biased when a substantial proportion of species are missing from samples [11]. Since similarity is a qualitative human construct and has no precise mathematical definition, all indices used to measure it inevitably hold some bias. For this reason, all the above-mentioned indices were used. Correspondence analysis based on Morisita similarity index was used in order to depict the differences of the prokaryotic communities along the sediment core.

The clone names used in this work indicate the sample site and library identification. The names begin with the letters AMSMV (as in Amsterdam MV), followed by a number showing the layer used to construct the library (0, 5, 10, 15, 20, 25, 30 cm.b.s.f.). The A or B character designates Archaea and Bacteria, respectively. The surface sampling was actually conducted in the 0–1-cm layer and, for simplicity reasons it is coded as 0 in the phylotype codes but annotated as 'surface layer' in the text.

Results

Geochemistry

The porewater sulfate concentration (Fig. 1) exhibited a decrease from bottom water values of near 30 mM to background values of less than 5 mM at ~22-cm sediment depth. The methane content was low in the topmost few centimetres, but rapidly increased with sediment depth from 13 to 27 cm.b.s.f. (Fig. 1).

Archaea

The archaeal clone libraries coverage (Fig. S1) according to Good's C estimator [37] was satisfactory (>0.8). A total of 339 Archaea 16S rRNA gene sequences were retrieved which were attributed to 55 phylotypes distributed in all sediment layers and 25 of them were unique for the whole core. Phylotypes grouped within the *Euryarchaeota* were the most abundant overall and the most abundant detected at each depth (Figs. 2, 3, S2).

Phylotypes belonging to ANME-1 group were retrieved in high abundances from all but 30 cm.b.s.f. libraries constructed. One ANME-1 phylotype was present at 0 (AMSMV-0-A18, 8.3%) and the same phylotype was retrieved at 5 cm.b.s.f. (as AMSMV-5-A10, 11.8%, Fig. 3). At 5 cm.b.s.f., two more phylotypes affiliated with ANME-1, AMSMV-5-A2 (23.5%) and AMSMV-5-A30 (2.0%) were found. ANME-1 phylotype AMSMV-0-A18 (or equivalently AMSMV-10-A33) dominated the 10-cm.b.s.f. layer, wherein comprised 54.6% of all Archaea clones sequenced in this library and 15-cm.b.s.f. layer (as AMSMV-15-A8, 45.5%).

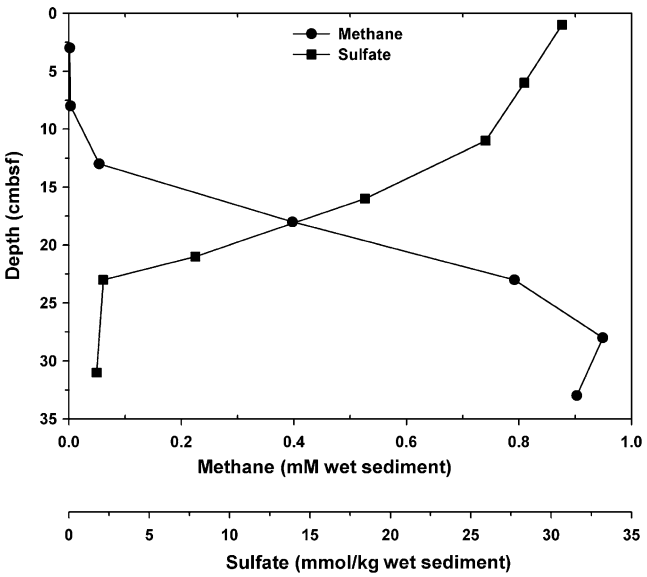

Figure 1 Vertical profile of methane and sulfate concentrations in the sediments of the Amsterdam mud volcano, East Mediterranean Sea

The same ANME-1 phylotype (AMSMV-20-A12, 32.8%) co-dominated 20 cm.b.s.f. together with AMSMV-0-A45 (or equivalently AMSMV-20-2, 31.0%) belonging to ANME-2a subgroup, and 25 cm.b.s.f. together with the ANME-2c, AMSMV-0-A12 (as AMSMV-25-A2, 39.1%).

The ANME-2 was the dominant group in the surface layer with AMSMV-0-A1 (Fig. 3), of the ANME-2b subgroup, the most abundant phylotype (37.5%). Two more ANME-2 phylotypes were found in the surface layer, AMSMV-0-A12 (16.7%) of ANME-2c subgroup and AMSMV-0-A45 (2.1%) of ANME-2a. At 5-cm.b.s.f. layer, AMSMV-0-A45 (as AMSMV-5-A3) became the dominate phylotype (31.4%) but AMSMV-0-A1 (as ANME-5-A7) was also present (19.6%). These phylotypes were retrieved from the 10-cm.b.s.f. layer, as well (AMSMV-0-A1 as ANME-10-A31, 25.4% and AMSMV-0-A45 as ANME-10-A35, 10.9%). The ANME-2a phylotype AMSMV-0-A45 was found at 15 cm.b.s.f. (AMSMV-15-A3, 9.1%) and 20 cm.b.s.f. (AMSMV-20-A2, 31.0%). At 20 cm.b.s.f., phylotype AMSMV-20-A2 (as AMSMV-5-A12) affiliated with group GoM Arc I, Gulf of Mexico Archaea I [44], formerly known as ANME-2d subgroup [48, 51], had significant representation (24.1%).

In the clone library from 30 cm.b.s.f., the dominant phylotype (70.8%), AMSMV-0-A33 (as AMSMV-30-A2), clustered within ANME-3 Euryarchaeota group (Fig. 3). This phylotype was also retrieved at 0 (AMSMV-0-33), 10 (AMSMV-10-A44) and 25 cm.b.s.f. (AMSMV-25-A12, but only with low abundance).

Phylotypes that grouped within MBG-D, Marine Benthic Group-D, (synonymous with marine group III—MG-III, a lineage within the *Thermoplasmatales*) were found at 0 (AMSMV-0-A22, 2.1% and AMSMV-0-A48, 2.1%), 25 cm.b.s.f. (AMSMV-25-A3, 6.5%) and 30 cm.b.s.f. (AMSMV-30-A53, 2.1%) layers.

All Crenarchaeota clones fell within MBG-B, Marine Benthic Group-B, (synonymous with deep-sea Archaea group). MBG-B Archaea exhibited high abundance at the surface layer (AMSMV-0-A10, 18.8% and AMSMV-0-A16 2.1%). Phylotypes belonging to MBG-B were also retrieved from 10 cm.b.s.f. (AMSMV-10-A48, 3.6%), 15 cm.b.s.f. (AMSMV-15-A7, 6.1%), 20 cm.b.s.f. (AMSMV-20-A17, 1.7%) and 25 cm.b.s.f. (AMSMV-25-A17, 2.2% and AMSMV-25-A24, 2.2%).

Phylotypes affiliated with the *Thaumarchaeota* (until recently characterised as Crenarchaeota clade MG 1—marine archaeal group 1) were present only in the surface layer. Three phylotypes were retrieved (AMSMV-0-A2, 2.2%, AMSMV-0-A34, 2.2% and AMSMV-0-A54, 2.2%).

Bacteria

The bacterial clone libraries' coverage (Fig. S1) according to Good's C estimator [37] was lower (ca. 0.4–0.8)

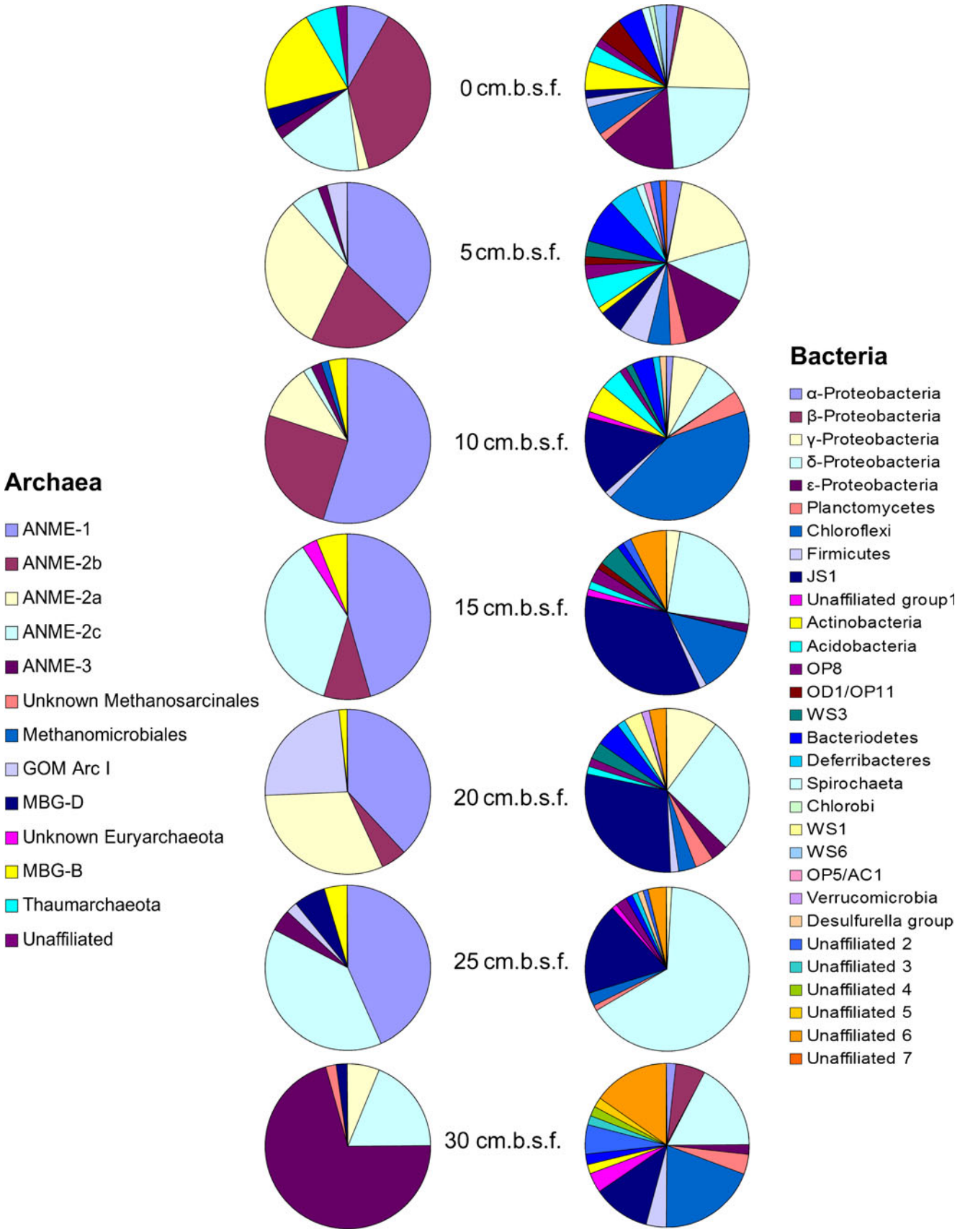

Figure 2 Relative abundance grouping of the found prokaryotic phylotypes from sediments of the Amsterdam mud volcano, East Mediterranean Sea. *cm.b.s.f.* cm below sea floor

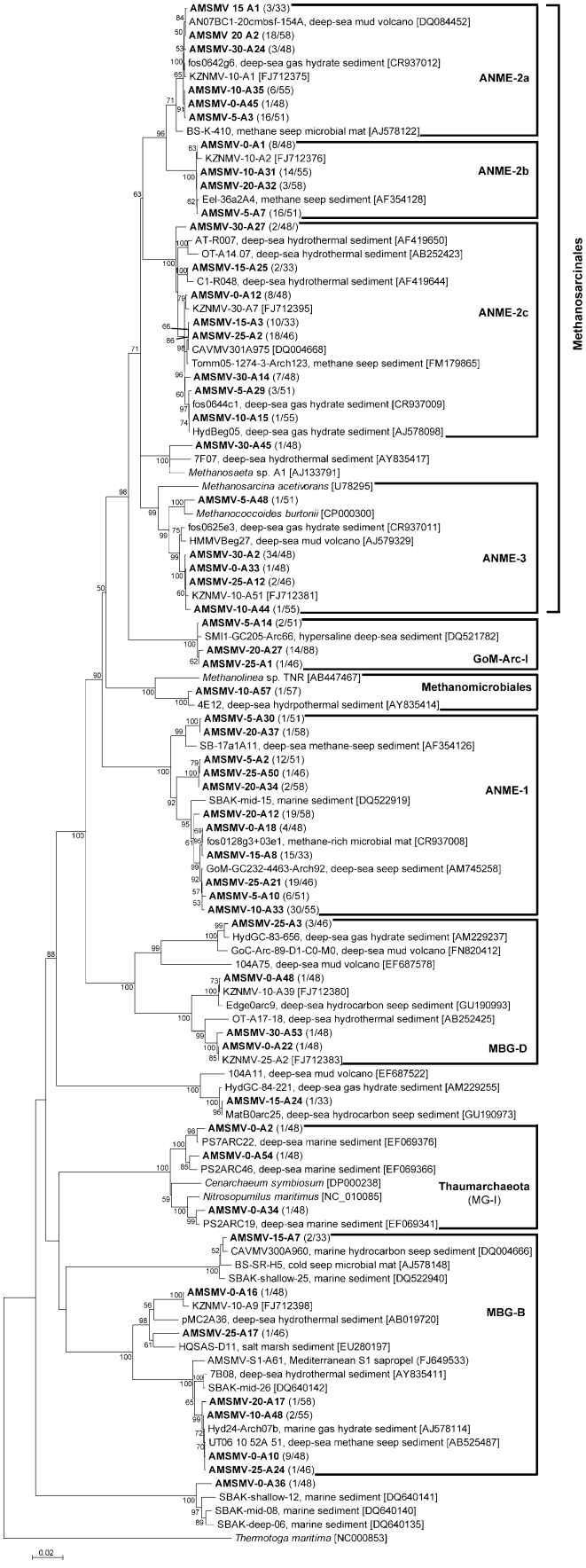

Figure 3 Phylogenetic tree of the Archaea 16S rRNA gene phylotypes (ca. 1,500 bp) in the sediments of the Amsterdam mud volcano, East Mediterranean Sea, based on the neighbour-joining method as determined by distance using Kimura's two-parameter correction. The found phylotypes (*bold letters*) are named after the sediment depth origin. *Numbers* of identical (≥98% sequence similarity) phylotypes of the total phylotype number in each sediment depth are shown in *parentheses*. One thousand bootstrap analyses (distance) were conducted, and percentages ≥50% are indicated at nodes. *Numbers in brackets* are GenBank accession numbers. *Scale bar* represents 2% estimated distance

compared to that for Archaea. A total of 526 bacterial 16S rRNA gene sequences were analysed and 276 phylotypes were identified in all sediment layers and 213 of them were unique. The majority of the retrieved clones were affiliated with *Proteobacteria* (Figs. 2, 4, S3, S4). The rest of the phylotypes were affiliated with: *Acidobacteria*, *Actinobacteria*, *Bacteriodetes*, *Chlorobi*, *Chloroflexi*, *Deferribacteres*, *Firmicutes*, *Planctomycetes*, *Spirochaetes*, *Verrucomicrobia*, candidate division JS1 [80], OD1/OP11 [27, 33], OP8 [33], WS1 [86], WS3 [19], WS6 [19], OP5, *Desulfurella* group [9] and seven unaffiliated groups (Fig. S5a, b, c).

At the surface layer phylotypes of δ- (23.1%) and γ- (22.3%) *Proteobacteria* co-dominated (Fig. 2). Phylotypes affiliated with *ε-Proteobacteria* exhibited high abundance (14.9%) and AMSMV-0-B65 (Fig. S3), the most abundant phylotype in this layer clusters within *ε-Proteobacteria* and is related to a phylotype reported from Kazan MV sediments. Representatives of *Actinobacteria* and *Chloroflexi* comprised 5.8% (each) of the total bacterial clones of the surface.

At 5 cm.b.s.f. *γ-Proteobacteria* showed the highest relative abundance (17.9%) followed by *δ-* and *ε-Proteobacteria*, which were retrieved in equal percentages (13.4%). The most abundant phylotype for this layer, AMSMV-0-B50 (as AMSMV-5-B2) clustered within *ε-Proteobacteria*, was also present at the surface layer and has previously been found in Kazan MV sediments. Phylotypes belonging to *Bacteriodetes* comprised 9.0% of the clone library from the 5-cm.b.s.f. layer and phylotypes belonging to *Chloroflexi* and *Firmicutes* appeared with relative abundance of 6.0%, each.

Phylotypes attributed to *Chloroflexi* dominated at 10 cm.b.s.f. (42.3%). At this sediment layer, *Proteobacteria* were found in a rather low relative abundance (7.0% for each one of the subdivision of *γ-* and *δ-Proteobacteria*). Phylotypes clustering within candidate division JS1 were present in all studied sediment layers. Based on the ≥98% similarity criterion they were found to represent the same phylotype. At the surface, AMSMV-0-B186 was retrieved at a relative abundance of 1.7%, and increased at 5 cm.b.s.f. (as AMSMV-5-B62, 4.5%). JS1 phylotype dominated at 10 cm.b.s.f. (as AMSMV-10-B11, 15.5%), 15 cm.b.s.f. (as AMSMV-15-B20, 34.8%) and 20 cm.b.s.f. (as AMSMV-20-B1, 28.8%). The relative abundance of this phylotype

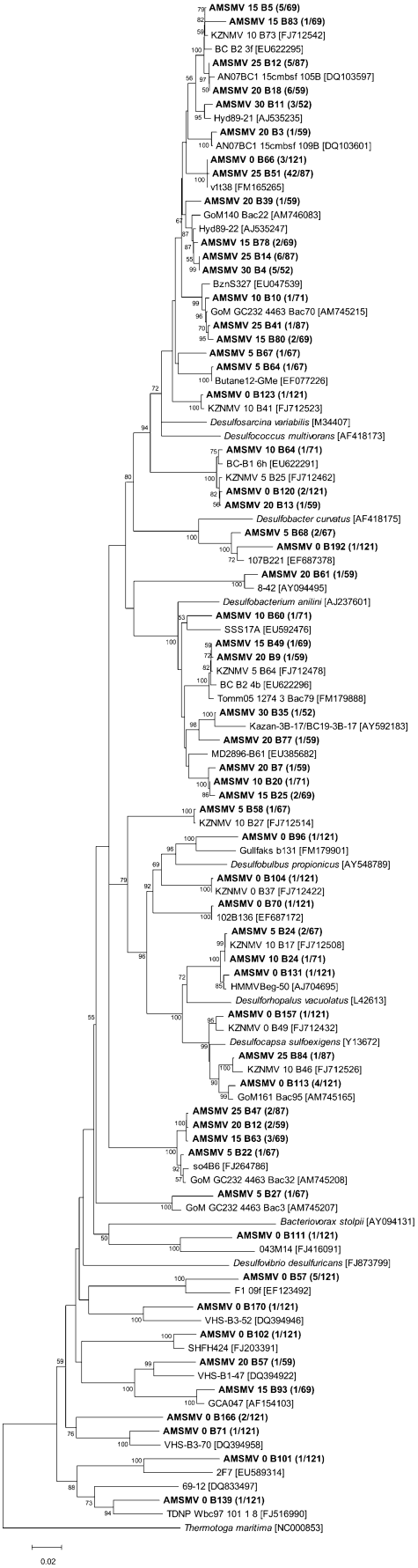

Figure 4 Phylogenetic tree of the *δ-Proteobacteria* 16S rRNA gene phylotypes (ca. 1,500 bp) in the sediments of the Amsterdam mud volcano, East Mediterranean Sea, based on the neighbour-joining method as determined by distance using Kimura's two-parameter correction. The found phylotypes (*bold letters*) are named after the sediment depth origin. Numbers of identical (≥98% sequence similarity) phylotypes of the total phylotype number in each sediment depth are shown in *parentheses*. One thousand bootstrap analyses (distance) were conducted, and percentages ≥50% are indicated at nodes. Numbers in brackets are GenBank accession numbers. *Scale bar* represents 2% estimated distance

decreased at 25 cm.b.s.f. (as AMSMV-25-B55, 18.4%) and further at 30 cm.b.s.f. (as AMSMV-30-B5, 11.6%).

Phylotypes of *δ-Proteobacteria* were retrieved at 15 and 20 cm.b.s.f. in relative abundances of 24.6% και 27.1%, respectively. *δ-Proteobacteria* was the dominant group at 25 cm.b.s.f. (65.6%) with AMSMV-0-B66 (as AMSMV-25-B51) the most abundant phylotype. The representation of *δ-Proteobacteria* was decreased at 30 cm.b.s.f. (17.3%). In that layer, phylotypes belonging to *Chloroflexi* dominated (19.2%).

Diversity and Similarity Indices

Shannon–Wiener diversity index H at all examined depths was higher for Bacteria (1.92–4.03) than for Archaea (0.99–1.91; Fig. 5). Changes in H with depth were not consistent between the Archaea and Bacteria clone libraries. The Archaea communities in AMSMV exhibited the lowest *H* value in the deepest studied sediment layer, 30 cm.b.s.f. and the highest in the surface layer. At 5 cm.b.s.f. *H* was 1.72, whilst the rest of the layers showed intermediate *H* values around 1.4. For Bacteria the highest *H* value appeared at the surface layer and *H* values for 5 and 10 cm.b.s.f. were also quite high (3.85 and 3.45, respectively). The lowest value was found at 25 cm.b.s.f..

The evenness index J (Fig. 5), followed approximately the same vertical profile with the diversity index, *H*. For Archaea, the highest *J* value was recorded at 5 cm.b.s.f. (0.829) and the lowest at 30 cm.b.s.f. (0.554). For Bacteria, *J* took high values (>0.9) at 0, 5 and 10 cm.b.s.f. and the lowest value at 25 cm.b.s.f. (0.639). The four different indices of similarity used are in agreement for most cases (Table S1). Setting the similarity threshold at 0.65 showed, for Bacteria, only one cluster of similar layers 15 and 20 cmbsf. The correspondence analysis (Fig. 6) revealed that these layers are also in close proximity to 25 and 30 cm.b.s.f., whilst 0, 5 and 10 cm.b.s.f. are distantly placed. Archaeal communities shared a greater degree of similarity. The sediment layers of 10, 15 and 20 cm.b.s.f. were found to form a cluster. Moreover, the 25-cm.b.s.f. layer seemed highly similar to the 15-cm.b.s.f. layer and 5 to 20 cm.b.s.f. (Fig. 6 and Table S1). The 30-cm.b.s.f. layer was highly dissimilar.

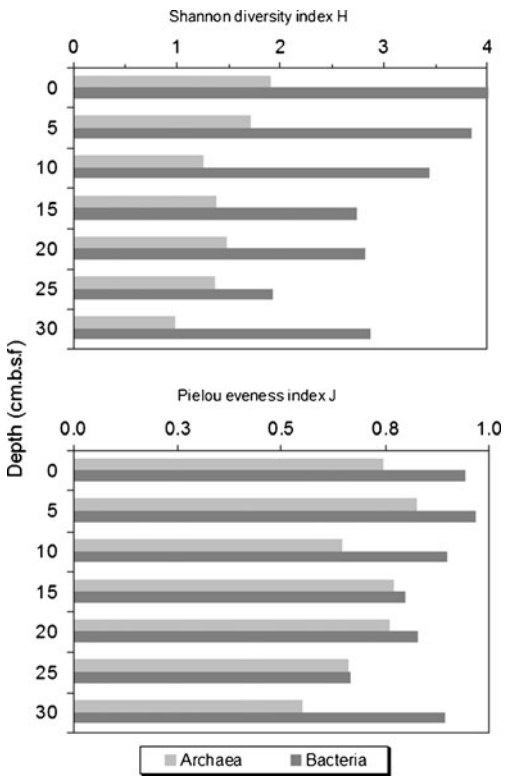

Figure 5 Shannon diversity index H and Pielou evenness index J for the Bacteria and Archaea 16S rRNA gene clone libraries from sediments of the Amsterdam mud volcano, East Mediterranean Sea

Phylotype comparison between AMSMV and Kazan mud volcano (KZNMV) revealed 12 and 36 common phylotypes for Archaea and Bacteria, respectively (Fig. S6). Eleven of the common Archaea phylotypes were exclusively found in mud volcanoes and related environments, with seven of those belonging to the ANME groups. Thirteen of the common Bacteria phylotypes belonged to sulfate-reducing *δ-Proteobacteria* and were similar to phylotypes from cold seeps. Seven phylotypes were attributed to *γ-Proteobacteria* related with putative sulfur and sulfide oxidizers. One phylotype was affiliated to the candidate division JS1. The rest of the common phylotypes belonged to the *α-* and *ε-Proteobacteria*, *Chloroflexi*, *Firmicutes*, *Bacteriodetes*, *Acidobacteria*, *Actinobacteria* and *Deferribacteres*.

Discussion

The clone library coverage indicated sampling saturation for the Archaea, implying that the majority of the Archaea phylotypes were revealed. The coverage for the Bacteria clone libraries was not as satisfactory as for the Archaea. Nevertheless, the most abundant bacterial phylotypes were retrieved, i.e., putative key players at the community level, and several 'rare' phylotypes (singletons and doubletons) as well. The use of the Shannon–Wiener diversity index *H* in prokaryotic communities is applicable and realistically informative [30, 37] especially when the clone library coverage is satisfactory. In our study, the Archaea clone libraries was satisfactory whilst for the Bacteria, although in most cases the coverage approached a plateau, the overall coverage was lower possibly due to the higher number of singletons and doubletons (Figs. S1, 3, S3, S5).

Archaea

Communities of Archaea in all layers were related to groups involved in methane metabolism. Phylotypes belonging to all three so far known ANME groups were found in high relative

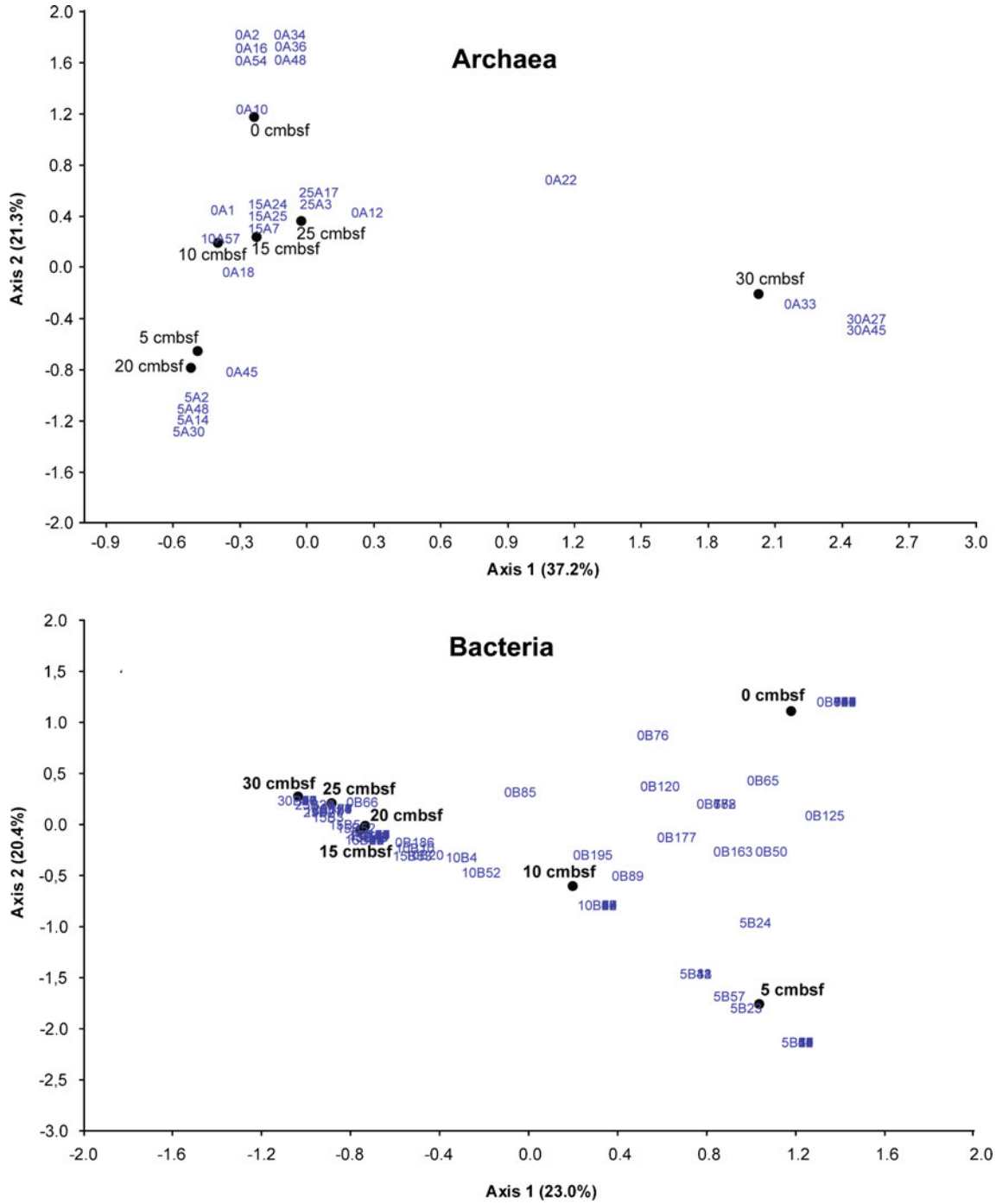

Figure 6 Correspondence analysis of the phylotype relative abundance for the Bacteria and Archaea 16S rRNA gene clone libraries from sediments of the Amsterdam mud volcano, East Mediterranean Sea. The unique phylotypes are shown in *blue letters*, where the sediment depth is depicted with the first number followed by *A* or *B* for Achaea and Bacteria, respectively, and the phylotype number; *cm.b.s.f.* cm below sea floor

abundances (>50% of all archaeal clones) in all depth layers. These yet-uncultivated *Euryarchaeota*, namely ANME-1, ANME-2 and ANME-3, are mediating AOM in marine environments, including other gas hydrate-bearing mud volcanoes [38 and references therein], and were differentially distributed along the investigated sediment layers.

Phylotypes of ANME-1 and ANME-2 groups were found to co-occur in most of the examined sediment layers, which is a rather common finding in AOM-related studies [18, 40, 51, 57] since it seems that, although phylogenetically distant, these groups perform AOM in a wide range of environmental settings. ANME-1 have been found to

dominate hypersaline sediments [44] or 'oily' sediments [54] from the Gulf of Mexico and microbial mats from the Black Sea [6, 49]. They can reach high abundances in deeper sediment layers and in microbial mats [28, 40, 55, 58], but in the sediment of AMSMV, their presence was unexpectedly high even in the top layers.

Since both ANME-1 and ANME-2 have been found in habitats with a wide range of methane concentrations and fluxes [44] it is possible that methane concentration is not the crucial factor for the selection of different groups. Instead, methane is believed to control total ANME biomass [14]. Other factors, such as salinity and oxygen presence, cannot sufficiently explain the relative abundance of either group. AMSMV sediments had low salinity but exhibited high-relative proportion of C_{2+} alkanes due to decomposition of structure II hydrates [61], which could fuel ANME-1 communities [54]. Moreover, ANME-1 and ANME-2 might perform AOM through different physiological mechanisms, with ANME-2 most likely to preferentially use sulfate as a mediator for AOM. ANME-1 cells, in some cases, have been observed in tight association with bacteria (e.g., microbial mats) but are most often found alone or in filaments, with no obvious syntrophic partnership as is the case for ANME-2 [40, 49, 56]. It is therefore also possible that they can mediate AOM in the absence of syntrophy. This has been calculated to be more energetically demanding [78] but methane oxidizers are believed to be adapted in chronic energy stress [77]. It is believed that ANME-1 might tolerate less favourable conditions for growth shaping more stable communities than ANME-2 [14].

ANME-3 is a less-studied group. ANME-3 have been found to dominate in sediments of the Haakon Mosby MV and believed to perform AOM either without obligatory physical association with a sulfate-reducing partner or with alternative partners [45]. The high abundance of ANME-3 at the 30-cm.b.s.f. horizon, where methane concentration is high (Fig. 1), might suggest that this group can effectively use high methane concentrations even without sulfate.

The presence of only a few *Thaumarchaeota*-related phylotypes, at the surface layer depicts a footprint of the overlying water column, as this group is known to play an important role in biogeochemical cycling in deep ocean waters [16, 36] and bathypelagic sediments [21]. The rest of the retrieved Archaea phylotypes, belonged to the GOM Arc I, MBG-D and MBG-C. These groups are generally associated with methane-rich environments, but their ecophysiological functions are still unknown [18, 40, 44, 75].

Bacteria

Communities of Bacteria showed much higher species richness and more complex structure. In total, the number of Bacteria phylotypes retrieved was more than five times higher than Archaea and was related to over 20 phylogenetic groups.

δ-Proteobacteria exhibited high relative abundance in almost all sediment layers. Sulfate-reducing *δ-Proteobacteria* phylotypes dominated the 25-cm.b.s.f. layer. The dominant phylotype AMSMV-25-B51 clustered within the *Desulfosarcina/Desulfococcus* group (SEEP-1) of *Desulfobacteriaceae*, syntrophic partners of ANME-1 and ANME-2 Archaea [7, 39, 49, 57, 67]. According to the geochemical profile, the 25-cm.b.s.f. horizon seems to be at the base of the sulfate reduction zone and it is possible that sulfate-reducing AOM takes place there. A few *Desulfobulbus*-like phylotypes were retrieved as well, implying versatility in bacterial partnership and AOM syntrophy [67].

High abundance (ca. 30%) of sulfate-reducing *δ-Proteobacteria* was also observed at 15 and 20 cm.b.s.f., as anticipated by the geochemical profile showing sulfate decrement. These layers showed high similarity implying that they share similar features which can shape similar Bacteria communities. Both of these layers showed high abundance of Bacteria groups that are not typically associated with AOM, such as the candidate division JS1 and *Chloroflexi*. JS1 was found in anoxic sedimentary habitats [80, 82] and is often associated with hydrate bearing and methane-rich sediments [34, 58]. *Chloroflexi* is a widespread group of Bacteria found in a diverse range of environments, not only subsurface sediments [15, 79] but also hot springs, hydrothermal sediments, soils, wastewater and polluted sites [33, 68, 74]. Within these two subsurface-related bacterial phyla there are no cultured members of JS1 and few cultured members of the *Chloroflexi*. For subsurface-related *Chloroflexi* it has been suggested that they anaerobically degrade recalcitrant carbon sources with H_2 consumption [83]. An insight of the physiology of JS1 was demonstrated [83] providing evidence of presence and activity under anaerobic sulfate-reducing conditions and ability of glucose (or glucose metabolites) and acetate utilisation. In the present study, the presence of the same JS1 phylotype in all sediment layers examined (and the dominance in most of them) clearly suggests a 'key-player' role for this phylotype in AMSMV sediments. The detection of a practically identical phylotype (>98% similarity) in sediments of Kazan MV (Fig. 3) and other methane-seep environments such as Hydrate Ridge and Gulf of Mexico sediments implies that its ecophysiology is related to sulfur cycle (see below).

The *ε-Proteobacteria* found in the AMSMV sediments belong to Marine Group I (MG I) [10], which includes phylotypes from deep-sea sediments, hydrothermal vents, sulfidic cave waters and cold seeps, phylogenetically associated with *Sulfurovum lithotrophicum* [35]. In addition to carbon cycling (due to CO_2 fixation [10, 25]), this cluster is oxidising sulfur and sulfidic compounds with nitrate or

oxygen, thus playing important role in the speciation of sulfur/nitrogen within a habitat. The majority of the retrieved *γ-Proteobacteria* in AMSMV was affiliated with sulfur and sulfide reducers and are expected to have similar impact in the sulfur cycling. The sulfur cycling is further corroborated by the high abundance of *δ-Proteobacteria*, since both groups can benefit from their complementary roles in sulfur cycling. Such co-occurrence has been reported before [62, 74] in hydrothermal sediments. Sulfate-reducing *δ-Proteobacteria* can utilise a wide spectrum of substrates which are being oxidised completely or incompletely to acetate, supplying their habitat with different forms of organic material (as well as reduced sulfur compound). These metabolic end-products could be used as substrates for growth by other microorganisms. There is evidence that a broad range of organisms can be active in an acetate slurry and able to use acetate directly or in close association with acetate utilizers [81]. Members of JS1, *Actinobacteria*, *α-Proteobacteria*, *Bacteriodetes*, *Firmicutes* and *Acidobacteria* have been associated with acetate incorporation in sulfate-reducing environments and that could explain the high abundance of these groups in AMSMV sediments. *Actinobacteria* are also know for their role in immobilising the dissolved organic matter and in degrading complex organic substrates such as lignin [71 and reference there in]. *Actinomycetes*, as well, have the ability to degrade recalcitrant organic matter [24]. Both of these groups may be critical players in controlling the degradation and mineralization of complex organic matter.

Planctomycetes can oxidise organic substrates through nitrate reduction [20], like *Pirellula* which is capable of heterolactic acid fermentation [22]. Moreover, members of *Planctomycetes* mediate anaerobic oxidation of ammonium [72], are abundant and important in the nitrogen cycle of Black Sea [42] and other suboxic marine waters and sediments [76]. The role of the deeply rooted Candidate Divisions OP8, WS3 and OD1/OP11 remains unknown. They have been exclusively found in marine ecosystems but their function remains doubtful. Representatives of OP8 in marine sediments were abundant in the iron/sulfate transition zone [19], as well as in hydrothermal fields and similar environments [62], whilst OP11 might be involved in the sulfur cycle [33].

The complexity of the prokaryotic community revealed by this study indicates that the process of AOM might involve more partners, than just a methanotroph archaeon and a sulfate-reducing bacterium. When there is adequate sulfate, methane is oxidised anaerobically by ANME acting in syntrophy with 'seep-specific' sulfate-reducing *δ-Proteobacteria* but the process could probably benefit from the participation of more groups that are able to use the products of AOM. Some of these groups (such as *α-*, *β-*, *γ-*, *ε-Proteobacteria*, *Planctomycetes* and *Bacteroidetes*) were found in association with the AOM consortium [63]. Sulfide oxidizers, members of *γ-* and *ε-Proteobacteria* can use the produced sulfide and refuel the sulfur cycle, whilst JS1 (and other groups) utilise acetate. Although we found several bacterial phylotypes which could be assigned only to the phylum level, it is possible that these unknown Bacteria could have active ecophysiological roles in AMSMV.

Diversity and Similarity Patterns

Archaea diversity was highest at the uppermost sediment layer, reflecting the contribution of the overlying water column to the Archaea community in the surface sediment, whilst diversity decreased throughout the depth of the core. At all sediment layers, the observed Archaea diversity was lower than the Bacteria, which is a general pattern in methane-related environments [29, 51, 66]. Bacterial communities in all but 15- and 20-cm.b.s.f. layers, appeared highly dissimilar, implying that a unique bacterial assemblage was established in each layer. Archaea communities, shared a greater degree of similarity. Only the surface and 30-cm.b.s.f. layer were different (Fig. 6). Although there is evidence of stratification (mainly for the bacterial communities), we observed continuous shifts of certain phylotype abundances for both Bacteria and Archaea implying that these communities are not totally isolated with each other and are partially overlapping in species composition.

Direct comparisons between analogue/similar habitats are seldom feasible due to different methodological approaches used, ranging from sampling to analysis of clone libraries, despite their usefulness especially in cases of unknown/uncultivated microorganisms prevail. The phylotypes found in the current study are directly comparable with those from the KZNMV [41, 58] since the methodologies used in both MV were exactly the same. Phylotype comparison (Fig. S6) between AMSMV and KZNMV revealed that in the two systems, 48.0% and 63.1%, respectively, of their Archaea phylotypes are common. Most of them belong to ANME or other groups metabolising methane and originate exclusively from MV and methane-rich sediment environments, where AOM is an active process. Bacteria shared a much lower number of common phylotypes between the two MV (16.7% and 19.2% for the AMSMV and KZNMV, respectively). Most of the common Bacteria phylotypes were sulfate-reducing *δ-Proteobacteria*, other sulfate-reducing partners for ANME performing AOM and the rest were affiliated with putative sulfur/sulfide oxidizers, groups that can metabolise intermediate products of sulfate mediated oxidation of methane or hydrocarbons (such as acetate utilizers), groups that can degrade complex organic material or groups with yet unknown ecophysiological role. Most of them exhibit significant similarity to clones from seep environments, associated bacterial phylotypes with AOM consortia [63] or

alternative bacterial partners for AOM [5]. Six of the Archaea (AMSMV-0-A12, -0-A18, -0-A22, -0-A33, -0-A45, -0-A48) and nine of the Bacteria (AMSMV-15-B5, -0-B66, -0-B186, -5-B23, -20-B3, -0-B123, -10-B9, -15-B49, -0-B195) phylotypes found in this study, were also found in Amsterdam and Kazan MV sediments sampled in 1998 [29]. Although MV and other cold-seep ecosystems are formed from dissimilar geological processes and fluid flow can vary considerably, resulting in temporal unpredictable variations in the concentrations of methane, sulfide and other porewater compounds [43], the occurrence of these common prokaryotic phylotypes (Fig. S6) suggests that these microorganisms could serve as 'foundation' species for similar environments and implies a degree of endemicity and functional redundancy for methane-based systems, such as mud volcanoes.

In conclusion, the prokaryotic communities at the sediments of the active site of the Amsterdam MV showed a stratified structure, with Bacteria communities being much more diverse but with Archaea having significantly more redundant functional roles. The majority of the found phylotypes were related to the expected AOM-related microorganisms but the found diversity of Bacteria indicated that other microorganisms with nitrogen- and sulfur-related metabolic pathways participate in these communities. A considerable fraction of the Archaea phylotypes, and a smaller number of Bacteria, was practically similar from the Kazan MV of the Anaximander MV, implying a degree of endemicity. At the scale of 5-cm sediment depth, it seems that the occurring communities share common phylotypes suggesting than MV communities should be seen as continua instead of isolated communities.

Acknowledgements This research project is co-financed by EU-European Social Fund (75%) and the Greek Ministry of Development-GSRT (25%). This work was partly supported by the European Commission projects ANAXIMANDER (contract no. EVK3-CT-2002-00068) and HERMIONE (contract no 226354). Captain, crew and participants of the R/V AEGAEO are gratefully acknowledged for their contribution to the field work, sampling and analyses. The authors thank the three anonymous reviewers for their valuable comments.

References

1. Aller JY, Aller RC, Kemp PF, Chistoserdov AY, Madrid VM (2010) Fluidized muds: a novel setting for the generation of biosphere diversity through geologic time. Geobiology 8:169–178
2. Aloisi G, Pierre C, Rouchy JM, Foucher JP, Woodside J (2000) Methane-related authigenic carbonates of Eastern Mediterranean Sea mud volcanoes and their possible relation to gas hydrate destabilisation. Earth Planet Sci Lett 184:321–338
3. Altschul SF, Gish W, Miller W, Myers EW, Lipman DJ (1990) Basic local alignment search tool. J Mol Biol 215:403–410
4. Ashelford KE, Chuzhanova NA, Fry JC, Jones AJ, Weightman AJ (2005) At least 1 in 20 16S rRNA sequence records currently held in public repositories is estimated to contain substantial anomalies. Appl Environ Microbiol 71:7724–7736
5. Beal EJ, House CH, Orphan VJ (2009) Manganese- and iron-dependent marine methane oxidation. Science 325:184–187
6. Blumenberg M, Seifert R, Reitner J, Pape T, Michaelis W (2004) Membrane lipid patterns typify distinct anaerobic methanotrophic consortia. Proc Natl Acad Sci USA 101:11111–11116
7. Boetius A, Ravenschlag K, Schubert CJ et al (2000) A marine microbial consortium apparently mediating anaerobic oxidation methane. Nature 407:623–626
8. Bouloubassi I, Aloisi G, Pancost RD et al (2006) Archaeal and bacterial lipids in authigenic carbonate crusts from Eastern Mediterranean mud volcanoes. Org Geochem 37:484–500
9. Burton NP, Norris PR (2000) Microbiology of acidic, geothermal springs of Montserrat: environmental rDNA analysis. Extremophiles 4:315–320
10. Campbell BJ, Engel AS, Porter ML, Takai K (2006) The versatile epsilon-proteobacteria: key players in sulphidic habitats. Nat Rev Microbiol 4:458–468
11. Chao A, Chazdon RL, Colwell RK, Shen TJ (2005) A new statistical approach for assessing similarity of species composition with incidence and abundance data. Ecol Lett 8:148–159
12. Charlou JL, Donval JP, Zitter T et al (2003) Evidence of methane venting and geochemistry of brines on mud volcanoes of the eastern Mediterranean Sea. Deep Sea Res I 50:941–958
13. Cita MB, Ryan WBF, Paggi L (1981) Prometheus mud-breccia: an example of shale diapirism in the Western Mediterranean Ridge. Ann Geo Pays Hellen 30:543–570
14. Constan L (2009) A correlation of anaerobic methane oxidizing archaea with geochemical gradients in Coastal Californian Marine sediments. Dissertation, The University of British Columbia
15. Coolen MJL, Cypionka H, Sass AM, Sass H, Overmann J (2002) Ongoing modification of Mediterranean pleistocene sapropels mediated by prokaryotes. Science 296:2407–2410
16. DeLong EF, Preston CM, Mincer T et al (2006) Community genomics among stratified microbial assemblages in the ocean \primes interior. Science 311:496–503
17. DeSantis TZ, Hugenholtz P, Keller K et al (2006) NAST: a multiple sequence alignment server for comparative analysis of 16S rRNA genes. Nucleic Acids Res 34:394–399
18. Dhillon A, Lever M, Lloyd KG et al (2005) Methanogen diversity evidenced by molecular characterization of methyl coenzyme M reductase A (*mcrA*) genes in hydrothermal sediments of the Guaymas Basin. Appl Environ Microbiol 71:4592–4601
19. Dojka MA, Hugenholtz P, Haack SK, Pace NR (1998) Microbial diversity in a hydrocarbon- and chlorinated-solvent- contaminated aquifer undergoing intrinsic bioremediation. Appl Environ Microbiol 64:3869–3877, 20
20. Fuerst JA (1995) The *Planctomycetes*: emerging models for microbial ecology, evolution and cell biology. Microbiology-UK 141:1493–1506
21. Gillan DC, Danis B (2007) The archaebacterial communities in Antarctic bathypelagic sediments. Deep Sea Res II 54:1682–1690
22. Glöckner FO, Kube M, Bauer M, Teeling H, Lombardot T, Ludwig W, Gade D, Beck A, Borzym K, Heitmann K, Rabus R, Schlesner H, Amann R, Reinhardt R (2003) Complete genome sequence of the marine planctomycete *Pirellula* sp. Strain 1. Proc Natl Acad Sci USA 100:8298–8303
23. Good IJ (1953) The population frequencies of species and the estimation of population parameters. Biometrika 40(3–4):237–264
24. Goodfellow M, Williams ST (1983) Ecology of actinomycetes. Annu Rev Microbiol 37:189–216

25. Grote J, Jost G, Labrenz M, Herndl GJ, Juergens K (2008) Epsilonproteobacteria represent the major portion of chemoautotrophic bacteria in sulfidic waters of pelagic redoxclines of the Baltic and Black Seas. Appl Environ Microbiol 74:7546–7551
26. Haese RR, Hensen C, De Lange GJ (2006) Pore water geochemistry of Eastern Mediterranean mud volcanoes: implications for fluid transport and fluid origin. Mar Geol 225:191–208
27. Harris JK, Kelley ST, Pace NR (2004) New perspective on uncultured bacterial phylogenetic division OP11. Appl Environ Microbiol 70:845–849
28. Harrison BK, Zhang H, Berelson W, Orphan VJ (2009) Variations in archaeal and bacterial diversity associated with the sulfate-methane transition zone in continental margin sediments (Santa Barbara Basin, California). Appl Environ Microbiol 75:1487–1499
29. Heijs SK, Laverman AM, Forney LJ, Hardoim PR, Van Elsas JD (2008) Comparison of deep-sea sediment microbial communities in the Eastern Mediterranean. FEMS Microbiol Ecol 64:362–377, 30
30. Hill TCJ, Walsh KA, Harris JA, Moffett BF (2003) Using ecological diversity measures with bacterial communities. FEMS Microbiol Ecol 43:1–11
31. Hinrichs KU, Hayes JM, Sylva SP, Brewert PG, DeLong EF (1999) Methane-consuming archaebacteria in marine sediments. Nature 398:802–805
32. Horn HS (1966) Measurement of "overlap" in comparative ecological studies. Am Nat 100:419–424
33. Hugenholtz P, Pitulle C, Hershberger KL, Pace NR (1998) Novel division level bacterial diversity in a Yellowstone hot spring. J Bacteriol 180:366–376
34. Inagaki F, Nunoura T, Nakagawa S et al (2006) Biogeographical Distribution and diversity of microbes in methane hydrate-bearing deep marine sediments on the Pacific Ocean margin. Proc Natl Acad Sci USA 103:2815–2820
35. Inagaki F, Takai K, Nealson KH, Horikoshi K (2004) *Sulfurovum lithotrophicum* gen. nov., sp. nov., a novel sulfur-oxidizing chemolithoautotroph within the *e-Proteobacteria* isolated from Okinawa trough hydrothermal sediments. Int J Syst Evol Microbiol 54:1477–1482
36. Karner MB, DeLong EF, Karl DM (2001) Archaeal dominance in the Mesopelagic Zone of the Pacific Ocean. Nature 409:507–510
37. Kemp PF, Aller JY (2004) Estimating prokaryotic diversity: when are 16S rDNA libraries large enough? Limnol Oceanogr Methods 2:114–125
38. Knittel K, Boetius A (2009) Anaerobic oxidation of methane: progress with an unknown process. Annu Rev Microbiol 63:311–334
39. Knittel K, Boetius A, Lemke A et al (2003) Activity, distribution, and diversity of sulfate reducers and other bacteria in sediments above gas hydrate (Cascadia margin, Oregon). Geomicrobiol J 20:269–294
40. Knittel K, Lösekann T, Boetius A, Kort R, Amann R (2005) Diversity and distribution of methanotrophic archaea at cold seeps. Appl Environ Microbiol 71:467–479
41. Kormas KA, Meziti A, Dählmann A, De Lange GJ, Lykousis V (2008) Characterization of methanogenic and prokaryotic assemblages based on mcrA and 16S rRNA gene diversity in sediments of the Kazan mud volcano (Mediterranean Sea). Geobiology 6:450–460
42. Kuypers MMM, Sliekers AO, Lavik G, Schmid M, Jorgensen BB, Kuenen JG, Damste JSS, Strous M, Jetten MSM (2003) Anaerobic ammonium oxidation by anammox bacteria in the Black Sea. Nature 422:608–611
43. Levin LA (2005) Ecology of cold seep sediments: interactions of fauna with flow, chemistry and microbes. CRC Press, Boca Raton
44. Lloyd KG, Lapham L, Teske A (2006) An anaerobic methane-oxidizing community of ANME-1b Archaea in hypersaline Gulf of Mexico sediments. Appl Environ Microbiol 72:7218–7230
45. Lösekann T, Knittel K, Nadalig T et al (2007) Diversity and abundance of aerobic and anaerobic methane oxidizers at the Haakon Mosby mud volcano, Barents Sea. Appl Environ Microbiol 73:3348–3362
46. Lykousis V, Alexandri S, Woodside J, de Lange G, Dählmann A, Perissoratis C, Heeschen K, Ioakim C, Sakellariou D, Nomikou P, Rousakis G, Casas D, Ballas D, Ercilla G (2009) Mud volcanoes and gas hydrates in the Anaximander Mountains (Eastern Mediterranean Sea). Mar Petrol Geol 26:854–872
47. Lykousis V, Alexandri S, Woodside J, Nomikou P, Perissoratis C, Sakellariou D, De Lange G, Dahlmann A, Casas D, Rousakis G, Ballas D, Ioakim C (2004) New evidence of extensive active mud volcanism in the Anaximander Mountains (Eastern Mediterranean): The "ATHINA" Mud Volcano. Environ Geol 46:1030–1037
48. Martinez RJ, Mills HJ, Story S, Sobecky PA (2006) Prokaryotic diversity and metabolically active microbial populations in sediments from an active mud volcano in the Gulf of Mexico. Environ Microbiol 8:1783–1796
49. Michaelis W, Seifert R, Nauhaus K et al (2002) Microbial reefs in the Black Sea fueled by anaerobic oxidation of methane. Science 297:1013–1015
50. Milkov AV (2000) Worldwide distribution of submarine mud volcanoes and associated gas hydrates. Mar Geol 167:29–42
51. Mills HJ, Martinez RJ, Story S, Sobecky PA (2005) Characterization of microbial community structure in Gulf of Mexico gas hydrates: comparative analysis of DNA- and RNA-derived clone libraries. Appl Environ Microbiol 71:3235–3247
52. Morisita M (1959) Measuring of interspecific association and similarity between communities. Mem Fac Sci Kyushu Univ Ser E (Biol) 3:65–80
53. Olu-Le Roy K, Sibuet M, Fiala-Médioni A et al (2004) Cold seep communities in the deep Eastern Mediterranean Sea: composition, symbiosis and spatial distribution on mud volcanoes. Deep Sea Res I 51:1915–1936
54. Orcutt BN, Joye SB, Kleindienst S, Knittel K, Ramette A, Reitz A, Samarkin V, Treude T, Boetius A (2010) Impact of natural oil and higher hydrocarbons on microbial diversity, distribution, and activity in Gulf of Mexico cold-seep sediments. DeepSea Res II 57:2008–2021
55. Orphan VJ, Hinrichs KU, Ussler Iii W, Paull CK, Taylor LT, Sylva SP, Hayes JM, Delong EF (2001) Comparative analysis of methane-oxidizing Archaea and sulfate-reducing bacteria in anoxic marine sediments. Appl Environ Microbiol 67:1922–1934
56. Orphan VJ, House CH, Hinrichs KU, McKeegan KD, DeLong EF (2001) Methane-consuming Archaea revealed by directly coupled isotopic and phylogenetic analysis. Science 293:484–487
57. Orphan VJ, House CH, Hinrichs KU, McKeegan KD, DeLong EF (2002) Multiple archaeal groups mediate methane oxidation in anoxic cold seep sediments. P Natl Acad Sci USA 99:7663–7668
58. Pachiadaki MG, Lykousis V, Stefanou EG, Kormas KA (2010) Prokaryotic community structure and diversity in the sediments of an active submarine mud volcano (Kazan mud volcano, East Mediterranean Sea). FEMS Microbiol Ecol 72:429–444
59. Pancost RD, Bouloubassi I, Aloisi G, Sinninghe Damsté JS (2001) Three series of non-isoprenoidal dialkyl glycerol diethers in cold-seep carbonate crusts. Org Geochem 32:695–707
60. Pancost RD, Sinninghe Damsté JS, De Lint S, Van Der Maarel MJEC, Gottschal JC (2000) Biomarker evidence for widespread anaerobic methane oxidation in mediterranean sediments by a consortium of methanogenic archaea and bacteria. Appl Environ Microbiol 66:1126–1132

61. Pape T, Kasten S, Zabel M, Bahr A, Abegg F, Hohnberg H-J, Bohrmann G (2010) Gas hydrates in shallow deposits of the Amsterdam mud volcano, Anaximander Mountains, Northeastern Mediterranean Sea. Geo Mar Lett 30:187–206
62. Perner M, Seifert R, Weber S, Koschinsky A, Schmidt K, Strauss H, Peters M, Haase K, Imhoff JF (2007) Microbial CO_2 fixation and sulfur cycling associated with low-temperature emissions at the Lilliput hydrothermal field, southern Mid-Atlantic Ridge. Environ Microbiol 9:1186–1201
63. Pernthaler A, Dekas AE, Brown CT, Goffredi SK, Embaye T, Orphan VJ (2008) Diverse syntrophic partnerships from deep-sea methane vents revealed by direct cell capture and metagenomics. P Natl Acad Sci USA 105:7052–7057
64. Pielou EC (1969) Association tests versus homogeneity tests: their use in subdividing quadrats into groups. Vegetatio 18:4–18
65. Pruesse E, Quast C, Knittel K, Fuchs BM, Ludwig W, Peplies J, Glöckner FO (2007) SILVA: a comprehensive online resource for quality checked and aligned ribosomal RNA sequence data compatible with ARB. Nucleic Acids Res 35:7188–7196
66. Reed AJ, Lutz RA, Vetriani C (2006) Vertical distribution and diversity of bacteria and archaea in sulfide and methane-rich cold seep sediments located at the base of the Florida Escarpment. Extremophiles 10:199–211
67. Schreiber L, Holler T, Knittel K, Meyerdierks A, Amann R (2010) Identification of the dominant sulfate-reducing bacterial partner of anaerobic methanotrophs of the ANME-2 clade. Environ Microbiol 12:2327–2340
68. Sekiguchi Y, Kamagata Y, Nakamura K, Ohashi A, Harada H (1999) Fluorescence in situ hybridization using 16S rRNA-targeted oligonucleotides reveals localization of methanogens and selected uncultured bacteria in mesophilic and thermophilic sludge granules. Appl Environ Microbiol 65:1280–1288
69. Shannon CE, Weaver W (1949) The mathematical theory of communication. University of Illinois Press, Urbana
70. Spiegelman D, Whissell G, Greer CW (2005) A survey of the methods for the characterization of microbial consortia and communities. Can J Microbiol 51:355–386
71. Stach EM, Bull A (2005) Estimating and comparing the diversity of marine actinobacteria. Antonie Leeuwenhoek 87:3–9
72. Strous M, Fuerst JA, Kramer EHM, Logemann S, Muyzer G, van de Pas-Schoonen KT, Webb R, Kuenen JG, Jetten MSM (1999) Missing lithotroph identified as new planctomycete. Nature 400:446–449
73. Tamura K, Dudley J, Nei M, Kumar S (2007) MEGA4: molecular evolutionary genetics analysis (MEGA) software version 4.0. Mol Biol Evol 24:1596–1599
74. Teske A, Hinrichs KU, Edgcomb V et al (2002) Microbial diversity of hydrothermal sediments in the Guaymas Basin: evidence for anaerobic methanotrophic communities. Appl Environ Microbiol 68:1994–2007
75. Teske A, Sørensen KB (2008) Uncultured archaea in deep marine subsurface sediments: have we caught them all? ISME J 2:3–18
76. Thamdrup B, Dalsgaard T (2002) Production of N_2 through anaerobic ammonium oxidation coupled to nitrate reduction in marine sediments. Appl Environ Microbiol 68:1312–1318
77. Valentine DL (2007) Adaptations to energy stress dictate the ecology and evolution of the archaea. Nat Rev Microbiol 5:316–323
78. Valentine DL, Reeburgh WS (2000) New perspectives on anaerobic methane oxidation. Environ Microbiol 2:477–484
79. Webster G, John Parkes R, Cragg BA, Newberry CJ, Weightman AJ, Fry JC (2006) Prokaryotic community composition and biogeochemical processes in deep subseafloor sediments from the Peru margin. FEMS Microbiol Ecol 58:65–85
80. Webster G, Parkes RJ, Fry JC, Weightman AJ (2004) Widespread occurrence of a novel division of bacteria identified by 16S rRNA gene sequences originally found in deep marine sediments. Appl Environ Microbiol 70:5708–5713
81. Webster G, Watt LC, Rinna J, Fry JC, Evershed RP, Parkes RJ, Weightman AJ (2006) A comparison of stable-isotope probing of DNA and phospholipid fatty acids to study prokaryotic functional diversity in sulfate-reducing marine sediment enrichment slurries. Environ Microbiol 8:1575–1589
82. Webster G, Yarram L, Freese E, Köster J, Sass H, Parkes RJ, Weightman AJ (2007) Distribution of candidate division JS1 and other bacteria in tidal sediments of the German Wadden Sea using targeted 16S rRNA gene PCR-DGGE. FEMS Microbiol Ecol 62:78–89
83. Wilms R, Köpke B, Sass H, Chang TS, Cypionka H, Engelen B (2006) Deep biosphere-related bacteria within the subsurface of tidal flat sediments. Environ Microbiol 8:709–719
84. Wolda H (1981) Similarity indices, sample size and diversity. Oecologia 50:296–302
85. Woodside JM, Ivanov MK et al (1998) Shallow gas and gas hydrates in the Anaximander Mountains region. Eastern Mediterranean Sea Gas hydrates: relevance to world margin stability and climate change Geol Soc Spec Publ 137:177–193
86. Zhou J, Davey ME, Figueras JB, Rivkina E, Gilichinsky D, Tiedje JM (1997) Phylogenetic diversity of a bacterial community determined from Siberian tundra soil DNA. Microbiology 143:3913–3919
87. Zitter TAC (2006) Mud volcanism and fluid emissions in Eastern Mediterranean neotectonic zones, VU University

SUPPLEMENTARY MATERIAL

Diversity and spatial distribution of prokaryotic communities along a sediment vertical profile of a deep-sea mud volcano

Maria G. Pachiadaki
Argyri Kallionaki
Anke Dählmann
Gert J. De Lange
Konstantinos Ar. Kormas*

"Microbial Ecology"
DOI:10.1007/s00248-011-9855-2

* E-mail: kkormas@uth.gr

Table S1. Similarity of Bacteria and Archaea sediment communities of the Amsterdam mud volcano, based on the indices of Morisita-Horn (first value), Morisita (second value), Jaccard adjusted (third value) and Sørensen adjusted (fourth value). Bold values indicate similar communities (≥0.650).

Bacteria

0 cm b.s.f.							
5 cm b.s.f.	0.327 0.606 0.142 0.249						
10 cm b.s.f.	0.125 0.165 0.170 0.291	0.247 0.386 0.350 0.519					
15 cm b.s.f.	0.078 0.088 0.131 0.232	0.205 0.245 0.169 0.290	0.553 0.637 0.170 0.291				
20 cm b.s.f.	0.098 0.118 0.233 0.378	0.209 0.266 0.141 0.248	0.537 0.647 0.153 0.265	**0.890** **0.998** 0.628 **0.772**			
25 cm b.s.f.	0.099 0.105 0.041 0.078	0.057 0.061 0.049 0.094	0.173 0.186 0.124 0.220	0.356 0.374 0.357 0.526	0.311 0.331 0.235 0.380		
30 cm b.s.f.	0.073 0.096 0.101 0.184	0.112 0.161 0.065 0.122	0.260 0.337 0.071 0.132	0.511 0.590 0.335 0.520	0.445 0.535 0.238 0.385	0.203 0.219 0.316 0.480	
	0 cm b.s.f.	*5 cm b.s.f.*	*10 cm b.s.f.*	*15 cm b.s.f.*	*20 cm b.s.f.*	*25 cm b.s.f.*	*30 cm b.s.f.*

Archaea

0 cm b.s.f.				
5 cm b.s.f.	0.468 0.506 0.575 0.730			
10 cm b.s.f.	0.519 0.545 **1.000** **1.000**	0.508 0.533 **0.677** **0.808**		
15 cm b.s.f.	0.341 0.368	0.379 0.408	**0.762** **0.800**	

	0.232	0.451	**0.672**				
	0.416	0.621	**0.804**				
	0.235	**0.686**	**0.704**	0.609			
20	0.250	**0.729**	**0.732**	0.648			
cm b.s.f.	**0.675**	**0.924**	**0.688**	0.417			
	0.806	**0.960**	**0.815**	0.588			
	0.383	0.285	**0.661**	0.947	0.474		
25	0.407	0.303	**0.686**	1.004	0.497		
cm b.s.f.	0.515	0.637	0.636	0.640	0.489		
	0.680	**0.778**	**0.778**	**0.780**	**0.657**		
	0.110	0.076	0.049	0.118	0.049	0.204	
30	0.114	0.079	0.051	0.123	0.050	0.210	
cm b.s.f.	0.239	0.154	0.146	0.158	0.055	0.405	
	0.386	0.267	0.254	0.273	0.104	0.576	
	0	*5*	*10*	*15*	*20*	*25*	*30*
	cm b.s.f.	*cm b.s.f.*	*cm b.s.f.*	*cm b.s.f.*	*cm b.s.f.*	*cm b.s.f.*	*cm b.s.f.*

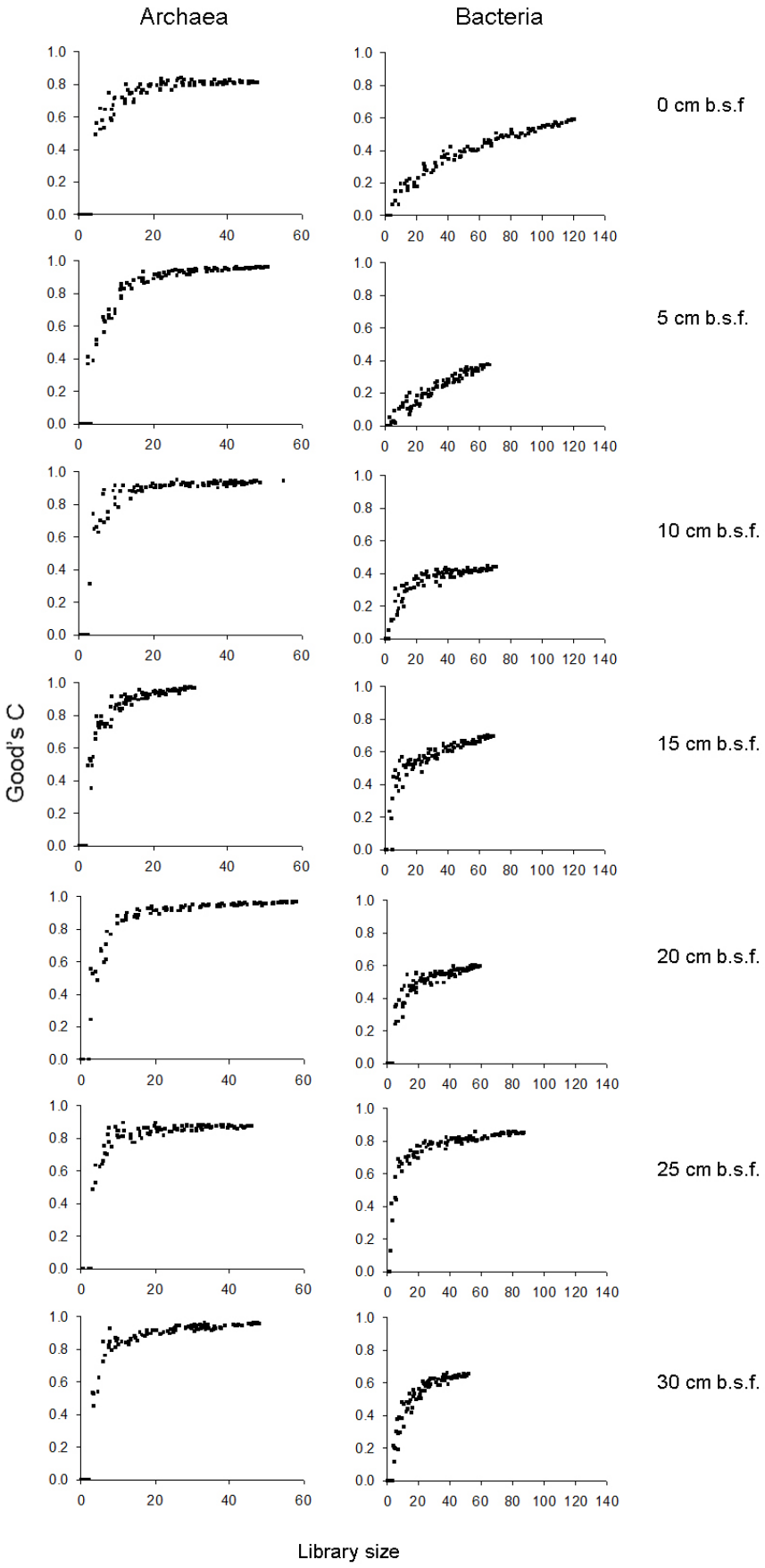

Figure S1. Clone library coverage based on Good's C estimator of the prokaryotic 16S rRNA gene libraries from the Amsterdam mud volcano, East Mediterranean Sea.

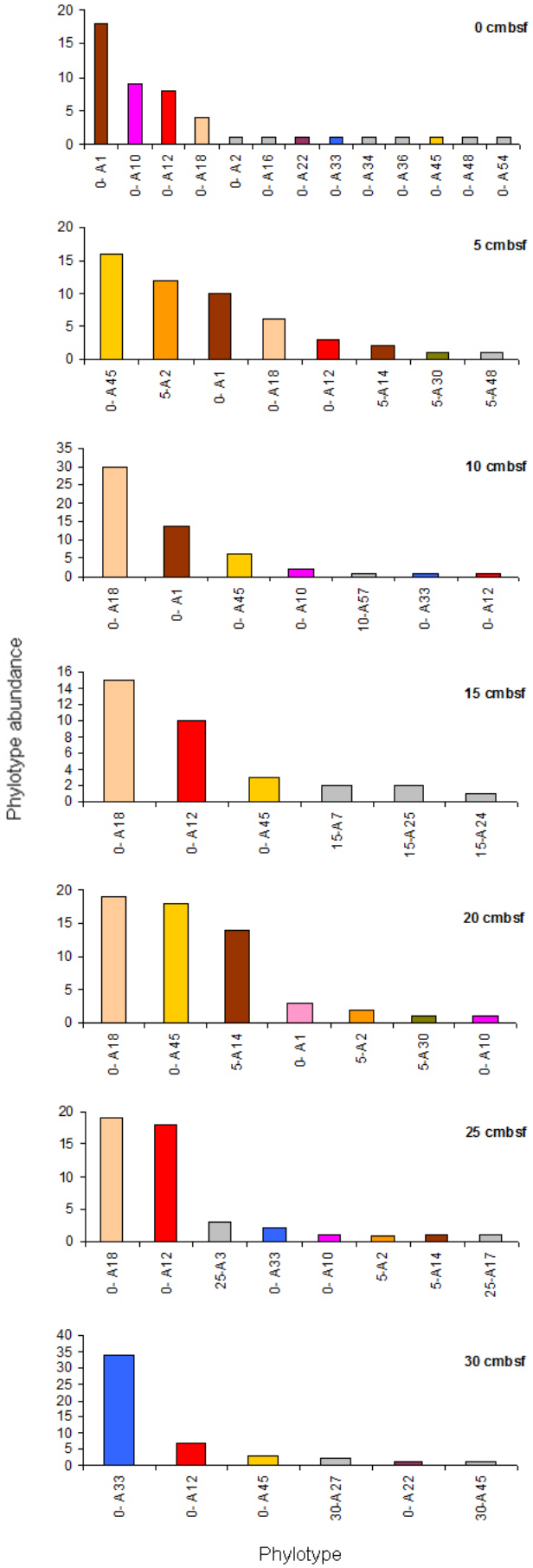

Figure S2. Occurrence of common Archaea phylotypes between the different sediment layers in the Amsterdam mud volcano, East Mediterranean Sea. The same colour corresponds to the same phylotype, while grey columns depict phylotypes that have occurred only at one layer.

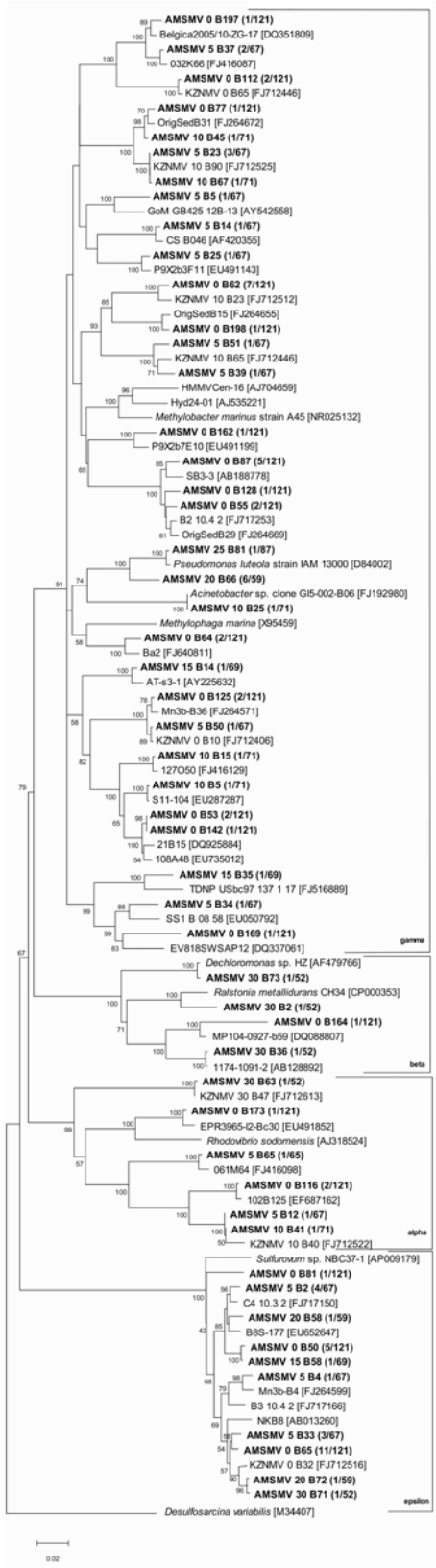

Figure S3. Phylogenetic tree of the α-, β-, γ- and ε-Proteobacteria 16S rRNA gene phylotypes (ca. 1500 bp) in the sediments of the Amsterdam mud volcano, East Mediterranean Sea, based on the neighbour-joining method as determined by distance using Kimura's two-parameter correction. The found phylotypes (bold letters) are named after the sediment depth origin. Numbers of identical (≥98% sequence similarity) phylotypes of the total phylotype number in each sediment depth are shown in parentheses. One thousand bootstrap analyses (distance) were conducted, and percentages ≥50% are indicated at nodes. Numbers in brackets are GenBank accession numbers. Scale bar represents 2% estimated distance.

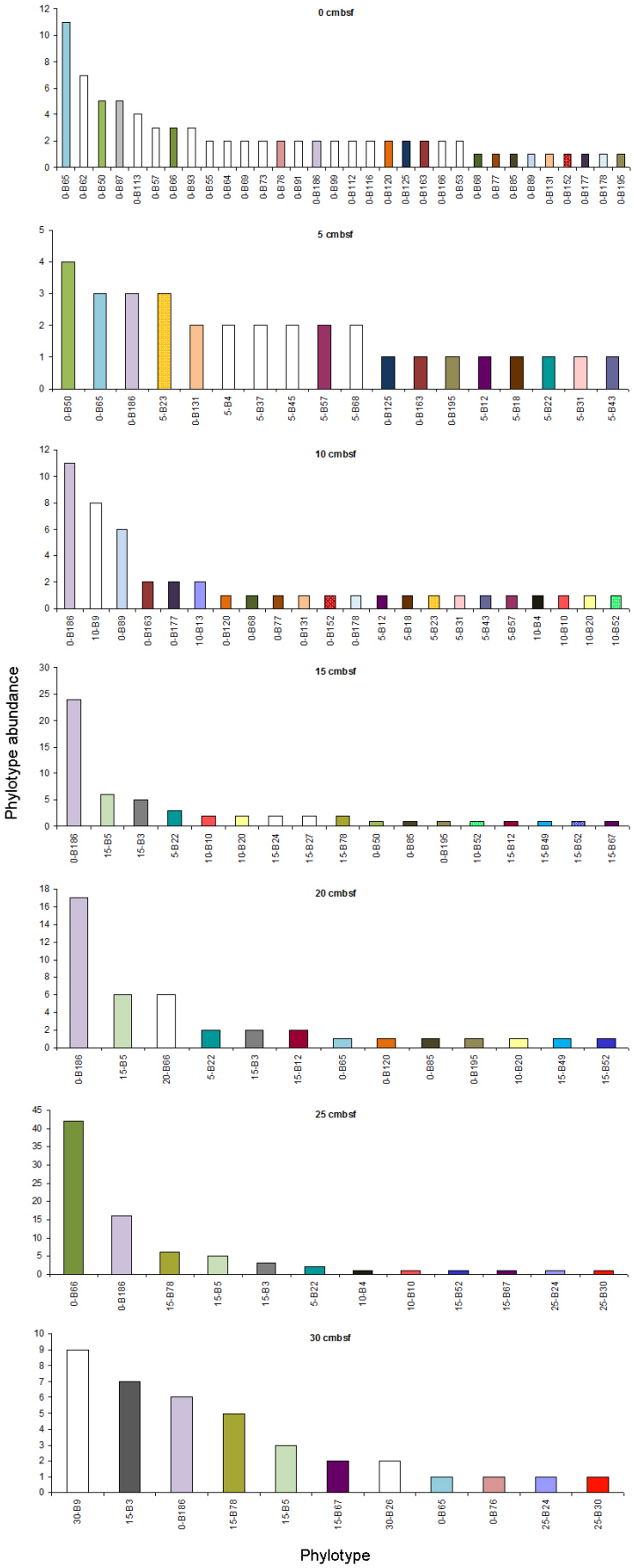

Figure S4. Occurrence of common Bacteria phylotypes between the different sediment layers in the Amsterdam mud volcano, East Mediterranean Sea. The same colour corresponds to the same phylotype, while blank columns depict phylotypes that have occurred only at one layer.

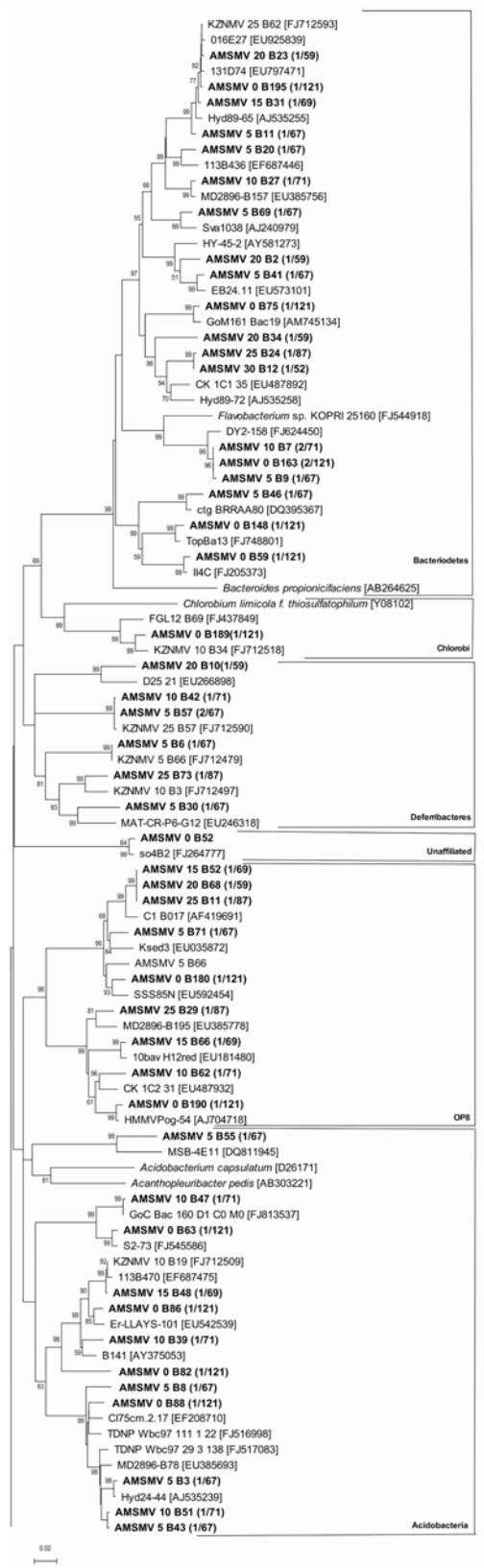

Figures S5a,b,c. Phylogenetic tree of the rest of the Bacteria 16S rRNA gene phylotypes (ca. 1500 bp) in the sediments of the Amsterdam mud volcano, East Mediterranean Sea, based on the neighbour-joining method as determined by distance using Kimura's two-parameter correction. The found phylotypes (bold letters) are named after the sediment depth origin. Numbers of identical (≥98% sequence similarity) phylotypes of the total phylotype number in each sediment depth are shown in parentheses. One thousand bootstrap analyses (distance) were conducted, and percentages ≥50% are indicated at nodes. Numbers in brackets are GenBank accession numbers. Scale bar represents 2% estimated distance.

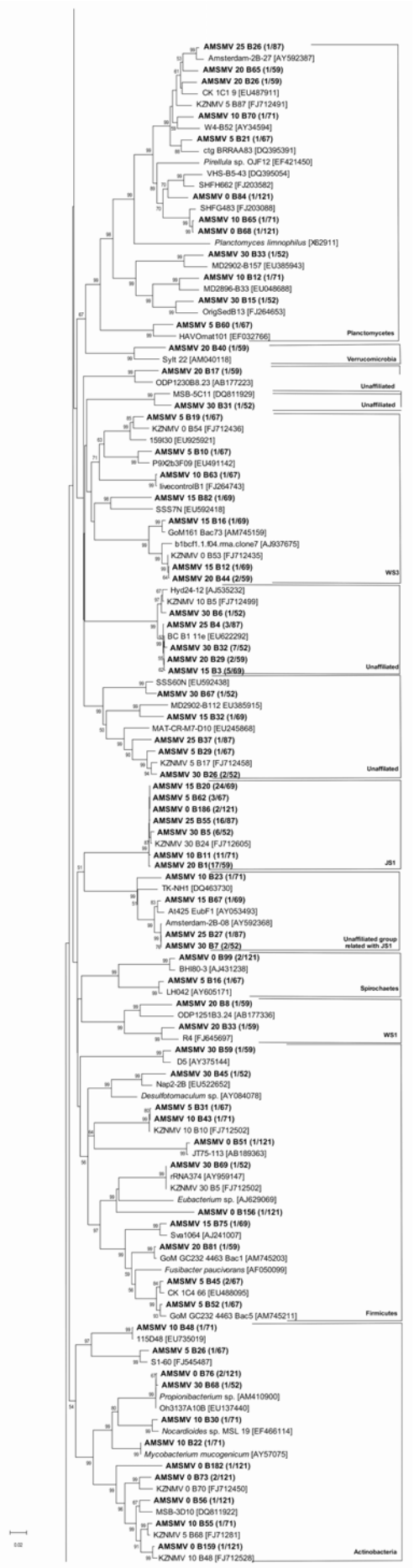
AMSMV 25 B26 (1/87)
Amsterdam-2B-27 [AY592387]
AMSMV 20 B65 (1/59)
AMSMV 20 B26 (1/59)
CK 1C1 9 [EU487911]
KZNMV 5 B87 [FJ712491]
AMSMV 10 B70 (1/71)
W4-B52 [AY34594]
AMSMV 5 B21 (1/67)
ctg BRRAA83 [DQ395391]
Pirellula sp. OJF12 [EF421450]
VHS-B5-43 [DQ395054]
SHFH662 [FJ203582]
AMSMV 0 B84 (1/121)
SHFG483 [FJ203088]
AMSMV 10 B65 (1/71)
AMSMV 0 B68 (1/121)
Planctomyces limnophilus [X62911]
AMSMV 30 B33 (1/52)
MD2902-B157 [EU385943]
AMSMV 10 B12 (1/71)
MD2896-B33 [EU048688]
AMSMV 30 B15 (1/52)
OrigSedB13 [FJ264653]
AMSMV 5 B60 (1/67)
HAVOmat101 [EF032766]
Planctomycetes
AMSMV 20 B40 (1/59)
Sylt 22 [AM040118]
Verrucomicrobia
AMSMV 20 B17 (1/59)
ODP1230B8.23 [AB177223]
Unaffiliated
MSB-5C11 [DQ811929]
AMSMV 30 B31 (1/52)
Unaffiliated
AMSMV 5 B19 (1/67)
KZNMV 0 B54 [FJ712436]
159I30 [EU925921]
AMSMV 5 B10 (1/67)
P9X2b3F09 [EU491142]
AMSMV 10 B63 (1/67)
livecontrolB1 [FJ264743]
AMSMV 15 B82 (1/69)
SSS7N [EU592418]
AMSMV 15 B16 (1/69)
GoM161 Bac73 [AM745159]
b1bcf1.1.f04.rma.clone7 [AJ937675]
KZNMV 0 B53 [FJ712435]
AMSMV 15 B12 (1/69)
AMSMV 20 B44 (2/59)
WS3
Hyd24-12 [AJ535232]
KZNMV 10 B5 [FJ712499]
AMSMV 30 B6 (1/52)
AMSMV 25 B4 (3/87)
BC B1 11e [EU622292]
AMSMV 30 B32 (7/52)
AMSMV 20 B29 (2/59)
AMSMV 15 B3 (5/69)
Unaffiliated
SSS60N [EU592438]
AMSMV 30 B67 (1/52)
MD2902-B112 EU385915]
AMSMV 15 B32 (1/69)
MAT-CR-M7-D10 [EU245868]
AMSMV 25 B37 (1/87)
AMSMV 5 B29 (1/67)
KZNMV 5 B17 [FJ712458]
AMSMV 30 B26 (2/52)
Unaffiliated
AMSMV 15 B20 (24/69)
AMSMV 5 B62 (3/67)
AMSMV 0 B186 (2/121)
AMSMV 25 B55 (16/87)
AMSMV 30 B5 (6/52)
KZNMV 30 B24 [FJ712605]
AMSMV 10 B11 (11/71)
AMSMV 20 B1(17/59)
JS1
AMSMV 10 B23 (1/71)
TK-NH1 [DQ463730]
AMSMV 15 B67 (1/69)
At425 EubF1 [AY053493]
Amsterdam-2B-08 [AY592368]
AMSMV 25 B27 (1/87)
AMSMV 30 B7 (2/52)
Unaffiliated group related with JS1
AMSMV 0 B99 (2/121)
BH180-3 [AJ431238]
AMSMV 5 B16 (1/67)
LH042 [AY605171]
Spirochaetes
AMSMV 20 B8 (1/59)
ODP1251B3.24 [AB177336]
AMSMV 20 B33 (1/59)
R4 [FJ645697]
WS1
AMSMV 30 B59 (1/59)
D5 [AY375144]
AMSMV 30 B45 (1/52)
Nap2-2B [EU522652]
Desulfotomaculum sp. [AY084078]
AMSMV 5 B31 (1/67)
AMSMV 10 B43 (1/71)
KZNMV 10 B10 [FJ712502]
AMSMV 0 B51 (1/121)
JT75-113 [AB189363]
AMSMV 30 B69 (1/52)
rRNA374 [AY959147]
KZNMV 30 B5 [FJ712502]
Eubacterium sp. [AJ629069]
AMSMV 0 B156 (1/121)
AMSMV 15 B75 (1/69)
Sva1064 [AJ241007]
AMSMV 20 B81 (1/59)
GoM GC232 4463 Bac1 [AM745203]
Fusibacter paucivorans [AF050099]
AMSMV 5 B45 (2/67)
CK 1C4 66 [EU488095]
AMSMV 5 B52 (1/67)
GoM GC232 4463 Bac5 [AM745211]
Firmicutes
AMSMV 10 B48 (1/71)
115D48 [EU735019]
AMSMV 5 B26 (1/67)
S1-60 [FJ545487]
AMSMV 0 B76 (2/121)
AMSMV 30 B68 (1/52)
Propionibacterium sp. [AM410900]
Oh3137A10B [EU137440]
AMSMV 10 B30 (1/71)
Nocardioides sp. MSL 19 [EF466114]
AMSMV 10 B22 (1/71)
Mycobacterium mucogenicum [AY57075]
AMSMV 0 B182 (1/121)
AMSMV 0 B73 (2/121)
KZNMV 0 B70 [FJ712450]
AMSMV 0 B56 (1/121)
MSB-3D10 [DQ811922]
AMSMV 10 B55 (1/71)
KZNMV 5 B68 [FJ71281]
AMSMV 0 B159 (1/121)
KZNMV 10 B48 [FJ712526]
Actinobacteria
0.02

Figure S5b

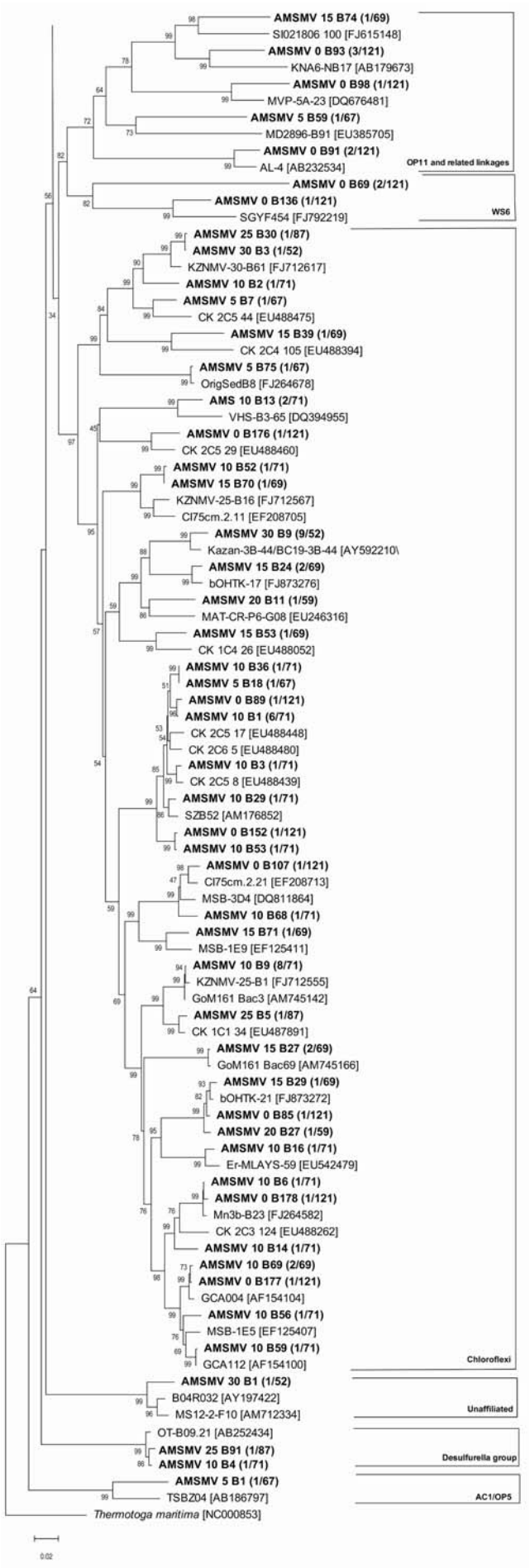
AMSMV 15 B74 (1/69)
SI021806 100 [FJ615148]
AMSMV 0 B93 (3/121)
KNA6-NB17 [AB179673]
AMSMV 0 B98 (1/121)
MVP-5A-23 [DQ676481]
AMSMV 5 B59 (1/67)
MD2896-B91 [EU385705]
AMSMV 0 B91 (2/121)
AL-4 [AB232534]
OP11 and related linkages
AMSMV 0 B69 (2/121)
AMSMV 0 B136 (1/121)
SGYF454 [FJ792219]
WS6
AMSMV 25 B30 (1/87)
AMSMV 30 B3 (1/52)
KZNMV-30-B61 [FJ712617]
AMSMV 10 B2 (1/71)
AMSMV 5 B7 (1/67)
CK 2C5 44 [EU488475]
AMSMV 15 B39 (1/69)
CK 2C4 105 [EU488394]
AMSMV 5 B75 (1/67)
OrigSedB8 [FJ264678]
AMS 10 B13 (2/71)
VHS-B3-65 [DQ394955]
AMSMV 0 B176 (1/121)
CK 2C5 29 [EU488460]
AMSMV 10 B52 (1/71)
AMSMV 15 B70 (1/69)
KZNMV-25-B16 [FJ712567]
CI75cm.2.11 [EF208705]
AMSMV 30 B9 (9/52)
Kazan-3B-44/BC19-3B-44 [AY592210\
AMSMV 15 B24 (2/69)
bOHTK-17 [FJ873276]
AMSMV 20 B11 (1/59)
MAT-CR-P6-G08 [EU246316]
AMSMV 15 B53 (1/69)
CK 1C4 26 [EU488052]
AMSMV 10 B36 (1/71)
AMSMV 5 B18 (1/67)
AMSMV 0 B89 (1/121)
AMSMV 10 B1 (6/71)
CK 2C5 17 [EU488448]
CK 2C6 5 [EU488480]
AMSMV 10 B3 (1/71)
CK 2C5 8 [EU488439]
AMSMV 10 B29 (1/71)
SZB52 [AM176852]
AMSMV 0 B152 (1/121)
AMSMV 10 B53 (1/71)
AMSMV 0 B107 (1/121)
CI75cm.2.21 [EF208713]
MSB-3D4 [DQ811864]
AMSMV 10 B68 (1/71)
AMSMV 15 B71 (1/69)
MSB-1E9 [EF125411]
AMSMV 10 B9 (8/71)
KZNMV-25-B1 [FJ712555]
GoM161 Bac3 [AM745142]
AMSMV 25 B5 (1/87)
CK 1C1 34 [EU487891]
AMSMV 15 B27 (2/69)
GoM161 Bac69 [AM745166]
AMSMV 15 B29 (1/69)
bOHTK-21 [FJ873272]
AMSMV 0 B85 (1/121)
AMSMV 20 B27 (1/59)
AMSMV 10 B16 (1/71)
Er-MLAYS-59 [EU542479]
AMSMV 10 B6 (1/71)
AMSMV 0 B178 (1/121)
Mn3b-B23 [FJ264582]
CK 2C3 124 [EU488262]
AMSMV 10 B14 (1/71)
AMSMV 10 B69 (2/69)
AMSMV 0 B177 (1/121)
GCA004 [AF154104]
AMSMV 10 B56 (1/71)
MSB-1E5 [EF125407]
AMSMV 10 B59 (1/71)
GCA112 [AF154100]
Chloroflexi
AMSMV 30 B1 (1/52)
B04R032 [AY197422]
MS12-2-F10 [AM712334]
Unaffiliated
OT-B09.21 [AB252434]
AMSMV 25 B91 (1/87)
AMSMV 10 B4 (1/71)
Desulfurella group
AMSMV 5 B1 (1/67)
TSBZ04 [AB186797]
AC1/OP5
Thermotoga maritima [NC000853]
0.02

Figure S5c

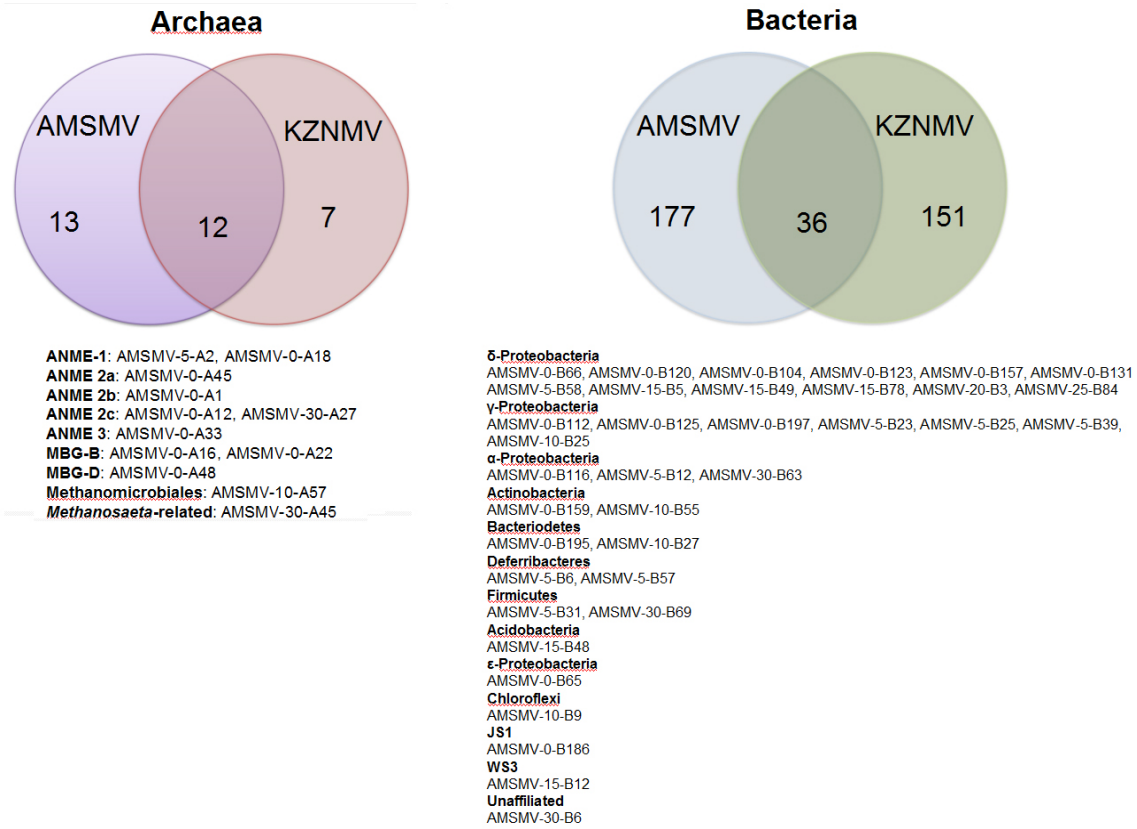

Figure S6. Venn diagrams of the common phylotypes (≥98%) between Amsterdam (AMSMV, this study) and Kazan (KZNMV) mud volcanoes. Data for the KZNMV are from Kormas et al. (2008) and Pachiadaki et al. (2010). The code names of the common phylotypes from each phylum are shown.